
Doctoral Dissertations

Student Theses and Dissertations

1973

Stability of the developing laminar flow in a circular tube

Lung-mau Huang

Follow this and additional works at: https://scholarsmine.mst.edu/doctoral_dissertations



Part of the [Mechanical Engineering Commons](#)

Department: **Mechanical and Aerospace Engineering**

Recommended Citation

Huang, Lung-mau, "Stability of the developing laminar flow in a circular tube" (1973). *Doctoral Dissertations*. 187.

https://scholarsmine.mst.edu/doctoral_dissertations/187

This thesis is brought to you by Scholars' Mine, a service of the Missouri S&T Library and Learning Resources. This work is protected by U. S. Copyright Law. Unauthorized use including reproduction for redistribution requires the permission of the copyright holder. For more information, please contact scholarsmine@mst.edu.

STABILITY OF THE DEVELOPING LAMINAR FLOW
IN A CIRCULAR TUBE

by

LUNG-MAU HUANG, 1940-

A DISSERTATION

Presented to the Faculty of the Graduate School of the

UNIVERSITY OF MISSOURI-ROLLA

In Partial Fulfillment of the Requirements for the Degree

DOCTOR OF PHILOSOPHY

in

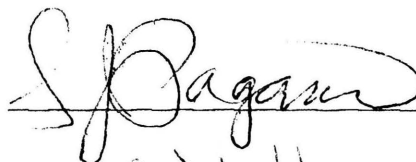
MECHANICAL ENGINEERING

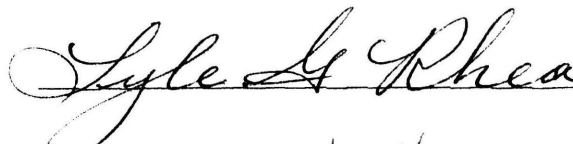
1973

T2788
111 pages
c.1



Advisor









237268

ABSTRACT

An investigation is made of the linear stability of the developing laminar flow of an incompressible fluid in the entrance region of a circular tube. Both axisymmetric and non-axisymmetric small disturbances are considered in the analysis. The stability characteristics of the fully developed flow are also re-examined. The main flow velocity distribution used in the stability analysis is that from the solution of the linearized momentum equation. The governing equations for the disturbances and the boundary conditions constitute an eigenvalue problem which is solved by a direct numerical integration scheme along with an iteration technique. The solution starts with a series expansion near the center of the tube, which is followed by a fourth order Runge-Kutta integration to the tube wall. Two purification methods, a filtering scheme and an orthonormalization technique, are used to remove the "parasitic errors" inherent in the numerical integration of the disturbance equations. Both purification schemes yield stability results which are essentially identical.

Neutral stability curves are generated and critical Reynolds numbers are obtained at various axial locations from the tube inlet for both axisymmetric disturbances and azimuthally periodic disturbances with periodicity one. Representative eigenfunctions are also presented. It is

found that: (1) laminar flow in the entrance region of a circular tube is unstable to both axisymmetric and azimuthally periodic disturbances; (2) the minimum critical Reynolds numbers occur in the entrance region and are about 20,000 (based on the average velocity and the radius of the tube) for both axisymmetric and azimuthally periodic disturbances; (3) the azimuthally periodic disturbances are more stable than the axisymmetric disturbances in the region adjacent to the entrance of the tube; and (4) in the region away from the tube inlet, the azimuthally periodic disturbances are more unstable than the axisymmetric disturbances. This last finding agrees with that of the earlier investigators for the fully developed flow.

ACKNOWLEDGMENT

The author wishes to express his sincere appreciation to his major advisor, Dr. T.S. Chen, for his guidance and encouragement. Professor Chen suggested this thesis topic and continually offered valuable comments and suggestions throughout the course of the investigation and during the preparation of the manuscripts. The many long hours of enlightening discussion with him, contributed greatly to the completion of the present work. Special thanks are also due to Dr. Lyle G. Rhea for his helpful assistance.

The author also wishes to thank Professor S.J. Pagano, Dr. C.Y. Ho and Dr. R.H. Howell for serving as other members of the examining committee.

The numerical phase of the work was made possible by funds from the Mechanical Engineering Department of the University of Missouri-Rolla.

Finally, the author expresses thanks to his wife, Pao-chu, for her understanding, patience, and encouragement throughout his graduate studies.

TABLE OF CONTENTS

	Page
ABSTRACT	ii
ACKNOWLEDGMENT	iv
LIST OF FIGURES.	vii
LIST OF TABLES	viii
NOMENCLATURE	x
I. INTRODUCTION	1
A. General Remarks.	1
B. Review of Previous Theoretical Investigations.	2
C. The Present Investigation.	5
II. MATHEMATICAL FORMULATION OF THE STABILITY PROBLEM.	9
A. The Main Flow.	9
B. Formulation of the Stability Problem	17
1. The Disturbance Equations.	17
2. Boundary Conditions.	24
3. The Eigenvalue Problem	26
III. THE NUMERICAL METHODS OF SOLUTION.	28
A. Introduction	28
B. The Starting Value for Numerical Integration	29
1. Axisymmetric Disturbances ($n=0$).	29
2. Non-Axisymmetric Disturbances with $n=1$	31
C. The Numerical Integration Schemes.	33
1. The Filtering Technique.	34
2. Gram-Schmidt Orthonormalization Procedure.	36
3. "Complete" Orthonormalization.	38

TABLE OF CONTENTS (continued)

	Page
D. Iteration Procedure for Determining the Eigenvalues.	39
E. Generation of the Neutral Stability Curve.	42
F. Calculation of Eigenfunctions.	45
IV. RESULTS AND DISCUSSION	49
A. The Eigenvalues.	49
B. The Effect of Stepsize on the Accuracy of Eigenvalues.	54
C. The Neutral Stability Curves	54
1. The Neutral Stability Curves for Axisymmetric Disturbances.	57
2. The Neutral Stability Curves for Non-Axisymmetric Disturbances.	61
D. Comparison of Results between Axisymmetric and Non-Axisymmetric Disturbances.	62
E. Eigenfunction.	68
V. CONCLUSION	76
REFERENCE.	78
VITA	82
APPENDICES	83
Appendix A. The Relationship among χ , ϵ and X	83
Appendix B. Tables of Neutral Stability Results for Axisymmetric Disturbances.	84
Appendix C. Tables of Neutral Stability Results for Non-Axisymmetric Disturbances.	90
Appendix D. Tables of Neutral Stability Characteristics at Critical Point.	97

LIST OF FIGURES

Figures	Page
1. The relationship among χ , ε and X	16
2. Neutral stability curves at various axial locations for axisymmetric disturbances $n=0$	59
3. Axial variation of critical Reynolds number for axisymmetric disturbances	60
4. Neutral stability curves at various axial locations for non-axisymmetric disturbances $n=1$	63
5. Axial variation of critical Reynolds number for non-axisymmetric disturbances	64
6. A comparison of neutral stability curves between axisymmetric and non-axisymmetric disturbances . . .	65
7. A comparison of axial variation of critical Reynolds number between axisymmetric and non-axisymmetric disturbances	67
8. Axial variation of critical wave number for axisymmetric and non-axisymmetric disturbances . . .	69
9. The eigenfunctions ϕ and ϕ' for $n=0$ at $\chi=0.006$; $\alpha=1.9$, $R=23781$, $c_r=0.346436$ and $c_i=0.0$	70
10. The eigenfunctions u , v and w for $n=1.0$ in fully developed region; $\alpha=0.98$, $R=2200$, $c_r=0.398348$ and $c_i=0.0678317$	71
11. The eigenfunctions u, v and w for $n=1.0$ at $\chi=0.006$; $\alpha=2.0$, $R=25009$, $c_r=0.325201$ and $c_i=0.0000166$. . .	74

LIST OF TABLES

Tables	Page
1. The Eigenvalues α_i	14
2. A Representative Comparison of Velocity Solution between Results from BESJ and the Polynomial Approximation ($\chi=0.003$)	15
3. A Comparison of Eigenvalue c Obtained from Various Techniques, $n=0$, $\alpha=1.0$, $R=5000$, $N=100$. . .	52
4. A Comparison of Eigenvalues for the Fully Developed Flow	53
5. A Comparison of Eigenvalues for the Developing Flow at $\chi=0.006$, $\alpha=1.9$, $R=23800$, $n=1.0$, and $N=150$	53
6. The Effect of Number of Steps on the Accuracy of Eigenvalues	55
7. Number of Steps Used in the Calculations at Various Axial Locations	56
8. Variation of Eigenvalues $c=c_r+c_i$ with α and R ($n=0$, $\chi=0.005$)	56
A-1. The Relationship among χ , ϵ and X	83
B-1. Neutral Stability Results for $n=0$ at $\chi=0.002$, $U_{max}=1.10722$, $N=200$	84
B-2. Neutral Stability Results for $n=0$ at $\chi=0.003$, $U_{max}=1.13312$, $N=200$	85
B-3. Neutral Stability Results for $n=0$ at $\chi=0.005$, $U_{max}=1.17564$, $N=150$	85
B-4. Neutral Stability Results for $n=0$ at $\chi=0.006$, $U_{max}=1.19420$, $N=150$	86
B-5. Neutral Stability Results for $n=0$ at $\chi=0.007$, $U_{max}=1.21157$, $N=150$	87
B-6. Neutral Stability Results for $n=0$ at $\chi=0.009$, $U_{max}=1.24367$, $N=150$	88

LIST OF TABLES (continued)

Tables	Page
B-7. Neutral Stability Results for $n=0$ at $\chi=0.010$, $U_{\max}=1.25870$, $N=100$	89
C-1. Neutral Stability Results for $n=1.0$ at $\chi=0.002$, $U_{\max}=1.10722$, $N=200$	90
C-2. Neutral Stability Results for $n=1.0$ at $\chi=0.003$, $U_{\max}=1.13312$, $N=200$	91
C-3. Neutral Stability Results for $n=1.0$ at $\chi=0.005$, $U_{\max}=1.17564$, $N=150$	92
C-4. Neutral Stability Results for $n=1.0$ at $\chi=0.006$, $U_{\max}=1.19420$, $N=150$	93
C-5. Neutral Stability Results for $n=1.0$ at $\chi=0.007$, $U_{\max}=1.21157$, $N=150$	94
C-6. Neutral Stability Results for $n=1.0$ at $\chi=0.009$, $U_{\max}=1.24367$, $N=150$	94
C-7. Neutral Stability Results for $n=1.0$ at $\chi=0.010$, $U_{\max}=1.25870$, $N=100$	95
C-8. Neutral Stability Results for $n=1.0$ at $\chi=0.015$, $U_{\max}=1.32702$, $N=100$	96
D-1. Axial Variation of Critical Stability Characteristics for Axisymmetric Disturbances $n=0$	97
D-2. Axial Variation of Critical Stability Characteristics for Non-Axisymmetric Disturbances $n=1.0$	98

NOMENCLATURE

a_i	coefficient appearing in equation (2-56)
A^i, B	matrixes defined in equations (3-23) and (3-24)
A_1, B_1	coefficients of equations (3-3), (3-9) and (3-10)
c	complex phase speed $c=c_r+c_i$
c_i, d_i	coefficients of the Frobenius series expansion in equations (3-1), (3-7) and (3-8)
E	secular equation (2-55) of the eigenvalue problem
F	operator in equation (3-15)
G	function defined in equation (3-32)
h	stepsize
J_i	Bessel function of the first kind of i th-order
L	operator in equations (2-19) through (2-22), and (2-26) through (2-29)
n	azimuthal periodicity or azimuthal wave number
N	number of steps used in numerical integration
$P^{(i)}$	upper triangular matrix, equation (3-38)
P_{ij}	elements of matrix $P^{(i)}$
q_i	component of base solution Q
Q	base solution
r	dimensionless radial coordinate
r^*	dimensional radial coordinate
r_0^*	radius of tube
R	Reynolds number based on maximum velocity, $R=u_{\max}^* r_0^*/\nu$

NOMENCLATURE (continued)

R^*	Reynolds number based on average velocity, $R^* = \bar{u}^* r_0^* / \nu$
t^*	dimensional time
t	dimensionless time
u^*, v^*, w^*, p^*	dimensional axial, radial and angular velocity components and pressure
u, v, w, p	dimensionless axial, radial and angular velocity components and pressure. also, amplitude functions of the disturbances for axial, radial and angular velocities and pressure
u^+, v^+, w^+, p^+	time dependent disturbances for axial, radial and angular velocities and pressure
$\bar{u}, \bar{v}, \bar{w}, \bar{p}$	dimensionless axial, radial and angular velocity components and pressure of mainflow
u_{\max}^*	dimensional maximum axial velocity of mainflow
\bar{u}^*	dimensional average velocity of mainflow
U	dimensionless mainflow velocity based on $u_{\max}^*, u^*/u_{\max}^*$
U_{\max}	dimensionless maximum velocity of mainflow, u_{\max}^*/\bar{u}^*
\bar{U}	dimensionless mainflow velocity based on \bar{u}^* , u^*/\bar{u}^*
\mathcal{V}	velocity vector

NOMENCLATURE (continued)

x^*	dimensional axial coordinate
X	dimensionless axial coordinate, $(x^*/r_0^*)/(\bar{u}^*r_0^*/\nu)$
y	function appearing in equation (3-42)
Z	orthonormalized independent solution, equation (3-37)
$w_{ii}, t^{(i)}, z^{(i)}$	defined in equation (3-39)
α_i	eigenvalues of equation (2-11)
$\beta^{(n)}$	coefficient matrix defined in equation (3-42)
β, γ	powers defined for Forbenius series expansion in equations (3-1), (3-7) and (3-8)
Δ	difference operator
ϵ	weighting function defined in equation (2-6)
θ	azimuthal coordinate
Λ	defined in equation (2-5)
ν	kinematic viscosity
ξ	dimensional stretched axial coordinate,
ρ	fluid density
ϕ, Ω	functions defined in equation (2-37) for non- axisymmetric disturbances
Φ	amplitude function of stream function for axisymmetric disturbances
χ	dimensionless stretched axial coordinate
ψ	stream function for axisymmetric disturbances
∇	gradient

NOMENCLATURE (continued)

∇^2 Laplacian operator

Subscripts

c critical condition
o condition at inlet of tube
g rapidly growing solution
s slowly growing solution
r real part
i imaginary part
~ vector

Superscript

' , " , ' ' , ' ' ' derivatives with respect to r

I. INTRODUCTION

A. General Remarks

In 1883 Reynolds (1) carried out systematic experiments and showed that the phenomenon of transition from laminar to turbulent flow in a circular tube occurs when the Reynolds number (based on the tube diameter and the average velocity) exceeds about 2,300. At the same time Rayleigh (2,3) started a series of theoretical studies on the inviscid stability of fluid flows to small disturbances. He discovered that velocity profiles which possess a point of inflection are unstable and that the speed of a neutral disturbance is smaller than the maximum main flow velocity. When Rayleigh's criterion is applied to fully developed pipe flow, the flow should be stable regardless of the Reynolds number. Later, Ekman (4) repeated Reynolds' experiments. He succeeded in maintaining laminar flow in a pipe up to a critical Reynolds number of 40,000 by providing an inlet which was made exceptionally free from disturbances.

Subsequently, the experimental investigations of Kuethe (5), Leite (6), Bhat (7) and Houlihan (8) showed that for Poiseuille pipe flow there exists a minimum critical Reynolds number of approximately 2,000, below which the flow remains laminar even in the presence of very strong disturbances.

In the theoretical investigations, the method of small disturbances has been successfully employed. This method

is based on the assumption that laminar flow is affected by certain infinitesimal disturbances (see, for example, Schlichting (9)). The behavior of small disturbances in a flow can be analyzed from the viewpoint of temporal stability or spatial stability. In the temporal stability analysis, disturbances which are periodic in axial distance are assumed to be applied at an initial instant everywhere in the fluid and are observed as time elapses. In the spatial stability analysis, disturbances which are periodic in time are imposed at a specified location in the fluid and are observed during their propagation downstream. The flow is considered to be stable, neutrally stable, or unstable depending on whether these disturbances are damped, remain constant, or amplified with respect to time for the temporal case or with respect to downstream distance for the spatial case, respectively.

B. Review of Previous Theoretical Investigations

The temporal stability of the fully developed flow in a pipe (i.e., the Poiseuille flow) to axisymmetric disturbances was analyzed theoretically by Sexl (10). However, his conclusions were unreliable since he applied some artificial boundary conditions for mathematical simplicity. Later, Pretsch (11) and Pekeris (12) found that there are two sets of solutions to the disturbances, one for the case of a disturbance confined to a thin region near the

wall and the other to a region near the center of the pipe. They are referred to, respectively, as the wall mode and the center mode solutions. Corcos and Sellars (13) studied these two sets of disturbances and reached a conclusion that only a finite number of eigenfunctions exist for the pipe flow stability problem. Schensted (14) subsequently showed that not only does a set of infinite eigenfunctions exist for the case of axisymmetric disturbances, but this set is complete. This problem has also been treated numerically by Davey and Drazin (15) using a direct integration technique. They found that the flow is stable to axisymmetric small disturbances.

Recently, Lessen, Sadler and Liu (16) used a numerical integration method to investigate the linear stability of pipe Poiseuille flow with respect to azimuthally periodic disturbances with periodicity $n=1$. Burrige (17) extended their work to cover different periodicities for the non-axisymmetric disturbances using numerical and asymptotic methods of solution. At the same time, Salwen and Grosch (18) found that the pipe flow is stable to infinitesimal disturbances in the range of azimuthal wave numbers $n=0,1,2,3,4,5$, axial wave numbers α between 0.1 and 10.0 and $\alpha R \leq 50,000$. These studies indicated that Poiseuille pipe flow is always temporally stable to infinitesimal disturbances of both axisymmetric and non-axisymmetric types. They also showed that the center mode disturbances are more unstable than the wall mode disturbances.

The spatial stability problem of pipe flow was analyzed by Gill (19). His theoretical results are in fair agreement with those of the experiments of Liete (6) and he concluded that the Poiseuille flow in a pipe is spatially stable to infinitesimal, axisymmetric disturbances. Garg and Rouleau (20) further extended Gill's work and found that up to Reynolds numbers of 10,000, the pipe Poiseuille flow is spatially stable to axisymmetric and non-axisymmetric, infinitesimal disturbances.

The theoretical investigations of Houlihan (8) and Graebel (21) have shown, on the other hand, that hydrodynamic instability of Poiseuille pipe flow exists for temporal, non-axisymmetrical small disturbances. By following the classical procedure of Tollmien, Houlihan found a portion of the neutral stability curve. However, he did not give a critical Reynolds number. Graebel's results from an asymptotic solution showed critical Reynolds number of 20 or larger. Since the findings of Houlihan and Graebel do not agree at all with those obtained from the numerical methods of solution, their results are open to question.

The temporal stability of laminar inlet-flow inside a circular tube due to small axisymmetric disturbances was investigated in great detail by Tatsumi (22) using an asymptotic series solution. He showed that instability of flow exists in the entrance section of a circular tube, and computed neutral stability curves for

wall mode disturbances at various distances downstream of the entrance. Tatsumi found that the critical Reynolds number decreases from infinity at tube inlet to a minimum with an increase in entrance length and then increases monotonically to infinity farther downstream.

C. The Present Investigation

From the previous studies, it can be concluded that Poiseuille pipe flow is stable to small disturbances of both axisymmetric and non-axisymmetric types. Furthermore, a comparison between the results of Davey and Drazin (15) and those of Burrige (17) shows that non-axisymmetric small disturbances with $n=1$ are more unstable than axisymmetric infinitesimal disturbances ($n=0$) for both wall and center modes. The instability of pipe flow to axisymmetric disturbances was found to occur in the entrance region. The question that needs to be answered is: Is the first instability in the development region of pipe flow due to axisymmetric disturbances or due to non-axisymmetric disturbances? This motivated the present investigation.

The present study deals with linear stability of the developing laminar flow in a circular tube. Both axisymmetric and azimuthally periodic, non-axisymmetric infinitesimal disturbances are considered in the analysis. The main objectives of the present investigation are fourfold. First, as pointed out by Chen (23), there

is an error in Tatsumi's work. In addition, in his stability calculation, Tatsumi applied the main flow profiles which were obtained under the assumption of "almost similarity" of the velocity profiles. These velocity profiles result in a description of the main flow which is inferior to other more recent representations. Thus, the results of Tatsumi are doubtful and there is a definite need to re-examine the stability characteristics of the developing tube flow to axisymmetric infinitesimal disturbances. Second, since in the fully developed flow, non-axisymmetric small disturbances with $n=1$ have been found to be more unstable than axisymmetric disturbances, it is of interest to study whether the developing pipe flow is more or less stable to non-axisymmetric disturbances with $n=1$ than to axisymmetric disturbances. Third, experimental work has shown that a critical Reynolds number exists in pipe flow. Previous theoretical investigation for the fully developed flow, on the other hand, showed that the flow is absolutely stable and thus no critical Reynolds number does exist. A comprehensive investigation of the flow instability in the entrance region of a pipe will, therefore, help clarify the existence or the lack of a critical Reynolds number. Fourth, it is of great importance to examine and compare the various numerical schemes employed in the stability calculations for pipe flow.

In the present study, consideration is given to the wall mode disturbances. In his study of the quasi-nonlinear

stability analysis for pipe flow, Chen (23) concluded that center mode disturbances merely flatten out the nose of the velocity profiles and probably contribute to a more stable flow. In fact, he found that the wall mode plays a more important role in the nonlinear instability of the flow. For the fully developed pipe flow, it has been found (16) that for large Reynolds numbers, both the least stable wall mode and the least stable center mode exhibit a stability characteristic which has almost the same amplification rate. In addition, in the entrance region of the tube, the main flow is of the boundary layer type and the instability of the flow, if it exists, should originate near the tube wall as in the boundary layer flow. For these reasons and for a comparison with Tatsumi's results, the present study is carried out for the wall mode. In the present investigation, the timewise stability characteristics are investigated using a numerical integration method of solution. A series solution for the stability equations near the center of the tube is obtained which serves as a starting point for the numerical integration. A direct numerical integration is then carried out to the tube wall. A filter technique (24) and an orthonormalization technique (25) are used to remove the "parasitic errors" inherent in the numerical integration.

Neutral stability curves at different axial locations in the entrance region are generated and the critical Reynolds numbers are determined for both axisymmetric and

non-axisymmetric disturbances. Representative results for the eigenfunctions are also presented. Finally, the stability results obtained with different methods of solution for these two cases are compared and discussed.

II. MATHEMATICAL FORMULATION OF THE STABILITY PROBLEM

A. The Main Flow

Before proceeding to the execution of the stability analysis, consideration is given to the main flow in the developing region of a circular tube. Of the various approximate analytical solutions available in the literature, the method of analysis carried out by Sparrow, Lin and Lundgren (26) appears to offer the most complete and accurate velocity distribution. With the linearization of the inertia terms in the momentum equation, they obtained velocity solutions which are continuous over the cross section and along the length from the entrance to the fully developed region. The advantage of employing this type of velocity profiles in the stability calculations is that the derivatives of velocity are continuous and can be obtained with great accuracy. It suffices here to give only the highlights of the linearization method used in finding the velocity solution for the main flow.

The basic equations governing laminar flow of an incompressible fluid are

Continuity equation

$$\nabla \cdot \underline{V} = 0 \quad 2-1$$

Momentum equation

$$\frac{\partial \underline{V}}{\partial t} + \underline{V} \cdot \nabla \underline{V} = -\frac{1}{\rho} \nabla p^* + \nu \nabla^2 \underline{V} \quad 2-2$$

where $V=(u^*,v^*,w^*)$ are the velocity component in the x^* , r^* , and θ directions, P^* is the pressure, ∇ and ∇^2 are, respectively, the gradient and Lapacian operators.

For the tube problem under consideration, the following assumptions are made: (1) the flow is steady, laminar and axisymmetric; (2) all fluid properties are constant; and (3) the Prandtl boundary layer assumptions apply. With these assumptions, equations (2-1) and (2-2) become, in cylindrical coordinates,

$$\frac{\partial u^*}{\partial x^*} + \frac{1}{r^*} \frac{\partial}{\partial r^*}(r^* v^*) = 0 \quad 2-3$$

and

$$u^* \frac{\partial u^*}{\partial x^*} + v^* \frac{\partial u^*}{\partial r^*} = -\frac{dP^*}{\rho dx^*} + \nu \left(\frac{\partial^2 u^*}{\partial r^{*2}} + \frac{1}{r^*} \frac{\partial u^*}{\partial r^*} \right) \quad 2-4$$

With application of the linearization method of Sparrow et al. (26), the momentum equation (2-4) is recast into the form

$$\varepsilon(x^*) \bar{u}^* \frac{\partial u^*}{\partial x^*} = \Lambda(x^*) + \nu \left(\frac{\partial^2 u^*}{\partial r^{*2}} + \frac{1}{r^*} \frac{\partial u^*}{\partial r^*} \right) \quad 2-5$$

in which $\varepsilon(x^*)$ is a weighting function of x^* to be determined. The function $\Lambda(x^*)$ is another undetermined function which includes the pressure gradient as well as the residual of the inertia terms.

A stretched axial coordinate ξ is introduced such that

$$dx^* = \varepsilon(\xi) d\xi \quad 2-6$$

Equation (2-5) is then integrated over the cross-section of the tube and the mass conservation is applied. This gives an expression for $\Lambda(x^*)$. Substitution of $\Lambda(x^*)$ back into equation (2-5) results in the dimensionless momentum equation

$$\frac{\partial \bar{U}}{\partial \chi} = \frac{\partial^2 \bar{U}}{\partial r^2} + \frac{1}{r} \frac{\partial \bar{U}}{\partial r} - 2 \left(\frac{\partial \bar{U}}{\partial r} \right)_{r=1} \quad 2-7$$

Which is to be solved subject to the boundary conditions

$$\bar{U} = 0 \text{ at } r=1.0, \quad \frac{\partial \bar{U}}{\partial r} = 0 \text{ at } r=0, \quad \bar{U} = 1.0 \text{ at } \chi=0 \quad 2-8$$

The dimensionless parameters in equation (2-7) are

$$\bar{U} = \frac{u^*}{\bar{u}^*}, \quad X = \frac{x^*/r_0^*}{\bar{u}^* r_0^*/\nu}, \quad \chi = \frac{\xi/r_0^*}{\bar{u}^* r_0^*/\nu}, \quad r = \frac{r^*}{r_0^*} \quad 2-9$$

in which \bar{u}^* is the average velocity, r_0^* is the radius of pipe, and ν is the kinematic viscosity. The velocity solution of equation (2-7) with boundary conditions (2-8) is given by

$$\bar{U} = 2(1 - r^2) + \sum_{i=1}^{\infty} \frac{4}{\alpha_i^2} \left\{ \frac{J_0(\alpha_i r)}{J_0(\alpha_i)} - 1 \right\} e^{-\alpha_i^2 \chi} \quad 2-10$$

Where the α_i are the positive roots of the equation

$$J_1(\alpha_i) = 0.5 \alpha_i J_0(\alpha_i), \quad i=1, 2, 3, \dots \quad 2-11$$

The solution given by equation (2-10) is still incomplete because the stretched axial coordinate χ appears instead of the physical axial coordinate X . The weighting function is evaluated under the assumption that the local pressure gradient calculated from momentum consideration be equal to the local pressure gradient obtained from mechanical energy consideration. This results in

$$\varepsilon = \frac{\int_0^1 (2\bar{U} - 1.5\bar{U}^2) (\partial\bar{U}/\partial\chi) r dr}{(\partial\bar{U}/\partial r)_{r=1} + \int_0^1 (\partial\bar{U}/\partial r)^2 r dr} \quad 2-12$$

Since $\bar{U} = \bar{U}(\chi, r)$, it is clear that the right-hand side of equation (2-12) is a function of χ only. The relationship between X and χ is expressed by

$$X = \int_0^X \varepsilon d\chi \quad 2-13$$

Thus, with $\varepsilon(\chi)$ specified, one can easily find the physical axial coordinate X from equation (2-13), and the velocity solution may then be considered as formally completed. A detailed solution method for \bar{U} is given in reference (26).

The eigenvalues α_i corresponding to the roots of equation (2-11) were found numerically by applying the computer subroutine DRTNI and a modified BESJ subroutine from the IBM Scientific Subroutine Package (27). The first 40 eigenvalues are listed in Table 1. It was found that less than 40 eigenvalues are needed to provide

numerical results with high accuracy even for the location $\chi=0.002$ which is very close to the tube inlet.

For the convenience of numerical calculations and without loss of accuracy, the polynomial approximation from Abramowitz and Stegan (28) is used instead of the subroutine BESJ to calculate the Bessel functions which appear in the velocity solution. At an axial location $\chi=0.003$, the velocity solution U (based on local maximum velocity) and its first and second derivatives with respect to r , U' and U'' , obtained with both methods are in good agreement as shown in Table 2.

The variation of the stretching factor ϵ with χ as calculated from equation (2-13) is presented in Figure 1 in which the ϵ is referred to the right-hand ordinate. It is seen from the figure that the ϵ value increases monotonically from a small value of 0.364 at the tube inlet with an increase in χ and approaches a limiting value of 1.82 as χ goes to infinity.

The relationship between X and χ is determined by carrying out the integration of ϵ as indicated in equation (2-13). The results are shown in Figure 1 where the X appears on the left-hand ordinate and χ on the abscissa. It is seen that, at locations near the entrance, X is less than χ . On the other hand, at larger downstream distances, the value of X exceeds that of χ . The numerical results for ϵ , X and χ are tabulated in Table A-1, Appendix A.

Table 1
 The Eigenvalues α_i
 $J_1(\alpha_i) = 0.5\alpha_i J_0(\alpha_i)$

i	α_i	i	α_i
1	5.1356223	21	68.302190
2	8.4172441	22	71.444990
3	11.619841	23	74.587688
4	14.795952	24	77.730297
5	17.959819	25	80.872827
6	21.116997	26	84.015287
7	24.270112	27	87.157684
8	27.420574	28	90.300025
9	30.569204	29	93.442316
10	33.716520	30	96.584561
11	36.862857	31	99.726744
12	40.008447	32	102.86893
13	43.153454	33	106.01107
14	46.297997	34	109.15317
15	49.442164	35	112.29524
16	52.586024	36	115.43729
17	55.729627	37	118.57931
18	58.873016	38	121.72131
19	62.016222	39	124.86329
20	65.159273	40	128.00525

Table 2

A Representative Comparison of Velocity Solutions
between Results from BESJ and the Polynomial Approxima-
tion ($\chi=0.003$)

r	U,U',U''	BESJ	Polynomial Approximation
0.15	U	0.99999734	0.99999735
	U'	-0.00001038	-0.00001039
	U''	0.00028585	0.00028226
0.65	U	0.99999049	0.99999049
	U'	-0.00042327	-0.00042325
	U''	-0.02444772	-0.02445027
0.75	U	0.99866949	0.99866949
	U'	-0.05921832	-0.05921853
	U''	-2.4352492	-2.4352526
0.85	U	0.94630774	0.94630771
	U'	-1.5872134	-1.5872133
	U''	-39.154516	-39.154506
0.95	U	0.48364390	0.48364394
	U'	-8.3095940	-8.3095948
	U''	-71.060492	-71.060520
0.975	U	0.25592315	0.25592316
	U'	-9.8032968	-9.8032969
	U''	-46.015765	-46.015773
1.0	U	0.0	0.0
	U'	-10.521900	-10.521897
	U''	-10.521906	-10.521902

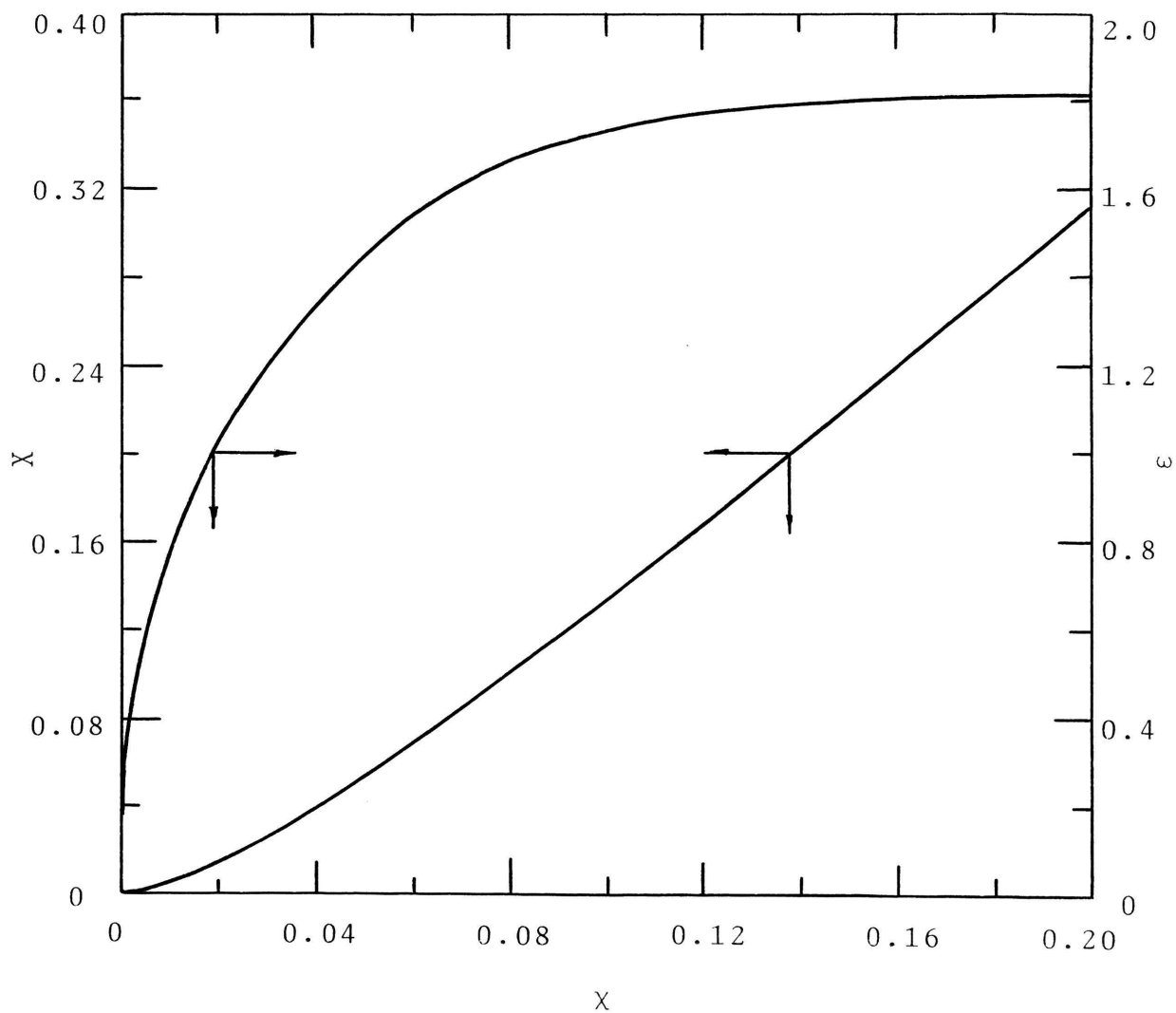


Figure 1. The relationship among χ , ϵ and X .

B. Formulation of the Stability Problem

In this section, the stability equations for the cases of axisymmetric and non-axisymmetric infinitesimal disturbances are formulated under certain conventional assumptions. The boundary conditions for each case are also discussed.

1. The Disturbance Equations

The basic equations governing laminar flow are the continuity and momentum equations. In formulating the disturbance equations, the following assumptions are made: (1) the fluid is newtonian with constant properties and the main flow is steady and incompressible; (2) the flow is parallel. This is not exactly the actual situation of the flow in the entrance region of the tube as encountered in the present problem. However, in situations in which the flow is nearly uni-directional, the parallel flow model is normally used for the purpose of stability analysis; (3) there are no body force; (4) the disturbances are infinitesimal; and (5) there is no slip at the tube wall. The equations of motion in cylindrical coordinates are:

Continuity equation:

$$\frac{\partial u^*}{\partial x^*} + \frac{\partial v^*}{\partial r^*} + \frac{v^*}{r^*} + \frac{1}{r^*} \frac{\partial w^*}{\partial \theta} = 0 \quad 2-14$$

Momentum equations (Navier-Stokes equations)

$$\begin{aligned} \frac{\partial u^*}{\partial t^*} + u^* \frac{\partial u^*}{\partial x^*} + v^* \frac{\partial u^*}{\partial r^*} + \frac{w^*}{r^*} \frac{\partial u^*}{\partial \theta} = - \frac{1}{\rho} \frac{\partial p^*}{\partial x^*} \\ + \nu \left(\frac{\partial^2 u^*}{\partial r^{*2}} + \frac{1}{r^*} \frac{\partial u^*}{\partial r^*} + \frac{1}{r^{*2}} \frac{\partial^2 u^*}{\partial \theta^2} + \frac{\partial^2 u^*}{\partial x^{*2}} \right) \end{aligned} \quad 2-15$$

$$\begin{aligned} \frac{\partial v^*}{\partial t^*} + u^* \frac{\partial v^*}{\partial x^*} + v^* \frac{\partial v^*}{\partial r^*} + \frac{w^*}{r^*} \frac{\partial v^*}{\partial \theta} - \frac{w^{*2}}{r^*} = - \frac{1}{\rho} \frac{\partial p^*}{\partial r^*} \\ + \nu \left(\frac{\partial^2 v^*}{\partial r^{*2}} + \frac{1}{r^*} \frac{\partial v^*}{\partial r^*} - \frac{v^*}{r^{*2}} + \frac{1}{r^{*2}} \frac{\partial^2 v^*}{\partial \theta^2} - \frac{2}{r^{*2}} \frac{\partial w^*}{\partial \theta} + \frac{\partial^2 v^*}{\partial x^{*2}} \right) \end{aligned} \quad 2-16$$

and

$$\begin{aligned} \frac{\partial w^*}{\partial t^*} + u^* \frac{\partial w^*}{\partial x^*} + v^* \frac{\partial w^*}{\partial r^*} + \frac{w^*}{r^*} \frac{\partial w^*}{\partial \theta} + \frac{w^* v^*}{r^*} = - \frac{1}{\rho} \frac{\partial p^*}{r^* \partial \theta} \\ + \nu \left(\frac{\partial^2 w^*}{\partial r^{*2}} + \frac{1}{r^*} \frac{\partial w^*}{\partial r^*} - \frac{w^*}{r^{*2}} + \frac{1}{r^{*2}} \frac{\partial^2 w^*}{\partial \theta^2} + \frac{2}{r^{*2}} \frac{\partial v^*}{\partial \theta} + \frac{\partial^2 w^*}{\partial x^{*2}} \right) \end{aligned} \quad 2-17$$

Equations (2-14) through (2-17) can be made dimensionless by choosing the radius of the tube r_0^* and the local maximum velocity u_{\max}^* as the characteristics length and velocity, respectively. By introducing the nondimensional variables

$$\begin{aligned} u &= u^*/u_{\max}^* , \quad v = v^*/u_{\max}^* , \quad w = w^*/u_{\max}^* , \\ x &= x^*/r_0^* , \quad r = r^*/r_0^* , \quad U = u^*/u_{\max}^* , \\ p &= p^*/\rho u_{\max}^{*2} , \quad t = t^* u_{\max}^*/r_0^* , \quad R = u_{\max}^* r_0^*/\nu , \end{aligned} \quad 2-18$$

into equations (2-14) through (2-17), one obtains the non-dimensional continuity and momentum equations.

$$\frac{\partial u}{\partial x} + \frac{1}{r} \frac{\partial}{\partial r} (rv) + \frac{1}{r} \frac{\partial w}{\partial \theta} = 0 \quad 2-19$$

$$\frac{\partial u}{\partial t} + u \frac{\partial u}{\partial x} + v \frac{\partial u}{\partial r} + \frac{w}{r} \frac{\partial u}{\partial \theta} = - \frac{\partial p}{\partial x} + \frac{1}{R} (Lu) \quad 2-20$$

$$\frac{\partial v}{\partial t} + u \frac{\partial v}{\partial x} + v \frac{\partial v}{\partial r} + \frac{w}{r} \frac{\partial v}{\partial \theta} - \frac{w^2}{r} = - \frac{\partial p}{\partial r} + \frac{1}{R} (Lv - \frac{v}{r^2} - \frac{2}{r^2} \frac{\partial w}{\partial \theta}) \quad 2-21$$

and

$$\frac{\partial w}{\partial t} + u \frac{\partial w}{\partial x} + v \frac{\partial w}{\partial r} + \frac{w}{r} \frac{\partial w}{\partial \theta} + \frac{vw}{r} = - \frac{1}{r} \frac{\partial p}{\partial \theta} + \frac{1}{R} (Lw - \frac{w}{r^2} + \frac{2}{r^2} \frac{\partial v}{\partial \theta}) \quad 2-22$$

where $L = \frac{\partial^2}{\partial x^2} + \frac{\partial^2}{\partial r^2} + \frac{\partial}{\partial r} \frac{1}{r} + \frac{\partial^2}{\partial r^2 \partial \theta^2}$.

In the stability analysis for parallel flow, the main flow has the form

$$\bar{u} = U(r) , \bar{v} = 0 , \bar{w} = 0 , \bar{p} = \bar{p}(x,r,\theta) , \quad 2-23$$

and the superimposed small disturbances are considered to be functions of time and space coordinates with the expressions

$$u^+(x,r,\theta,t) , v^+(x,r,\theta,t) , w^+(x,r,\theta,t) , p^+(x,r,\theta,t) \quad 2-24$$

The resultant motion is, therefore, described by

$$u = U + u^+ , v = v^+ , w = w^+ , p = \bar{p} + p^+ \quad 2-25$$

Substituting equation (2-25) into equations (2-19) through (2-22), and neglecting the quadratic terms in the

disturbance components, one obtains the equation of continuity for the perturbation

$$\frac{\partial u^+}{\partial x} + \frac{1}{r} \frac{\partial}{\partial r}(rv^+) + \frac{1}{r} \frac{\partial w^+}{\partial \theta} = 0 \quad 2-26$$

and the perturbation equations of motion

$$\frac{\partial u^+}{\partial t} + U \frac{\partial u^+}{\partial x} + v^+ \frac{\partial U}{\partial r} = - \frac{\partial p^+}{\partial x} + \frac{1}{R}(Lu^+) \quad 2-27$$

$$\frac{\partial v^+}{\partial t} + U \frac{\partial v^+}{\partial x} = - \frac{\partial p^+}{\partial r} + \frac{1}{R}(Lv^+ - \frac{v^+}{r^2} - \frac{2}{r^2} \frac{\partial w^+}{\partial \theta}) \quad 2-28$$

and

$$\frac{\partial w^+}{\partial t} + U \frac{\partial w^+}{\partial x} = - \frac{1}{r} \frac{\partial p^+}{\partial \theta} + \frac{1}{R}(Lw^+ - \frac{w^+}{r^2} + \frac{2}{r^2} \frac{\partial v^+}{\partial \theta}) \quad 2-29$$

where $L = \frac{\partial^2}{\partial x^2} + \frac{\partial^2}{\partial r^2} + \frac{\partial}{\partial r} / r \frac{\partial}{\partial r} + \frac{\partial^2}{\partial \theta^2} / r^2$.

Since the main flow is parallel, the steady-state solution is independent of the coordinates x , θ and t . Thus, the normal modes for disturbances will involve these coordinates exponentially. This can be shown by taking Fourier and Laplace transformations of the above equations (2-26) through (2-29). It can, therefore, be assumed that equations (2-26), (2-27), (2-28) and (2-29) have solutions of the form

$$\begin{pmatrix} u^+ \\ v^+ \\ w^+ \\ p^+ \end{pmatrix} = \begin{pmatrix} u(r) \\ v(r) \\ w(r) \\ p(r) \end{pmatrix} \exp\{i(\alpha x + n\theta - \alpha ct)\} \quad 2-30$$

where α is the axial wave number, n is the azimuthal wave

number, and $c=c_r+ic_i$ is the complex phase speed, with c_r denoting the phase speed of disturbances and c_i the damping or amplification factor for the disturbances.

Substituting equation (2-30) into the perturbation equation of continuity and the perturbation equations of motion, one obtains the following linearized ordinary differential equations in terms of the dimensionless amplitude functions u,v,w of the disturbances

$$i\alpha u + v' + v/r + inw/r = 0 \quad 2-31$$

$$i\alpha R(U - c)u + RU'v = - i\alpha Rp + u'' + u'/r - (n^2/r^2 + \alpha^2)u \quad 2-32$$

$$i\alpha R(U - c)v = -Rp' + v'' + v'/r - \{(n^2+1)/r^2 + \alpha^2\}v - i2nw/r^2 \quad 2-33$$

and

$$i\alpha R(U - c)w = - inRp/r + w'' + w'/r - \{(n^2+1)/r^2 + \alpha^2\}w + i2nv/r^2 \quad 2-34$$

where the primes denote differentiation with respect to r .

Equations (2-31) through (2-34) can be transformed into the following coupled equations by eliminating the pressure terms and after some rearrangements (see Burridge (17)).

$$\begin{aligned}
& \frac{1}{i\alpha R} \left\{ \phi'''' + \frac{2(n^2 - \alpha^2 r^2)}{r(n^2 + \alpha^2 r^2)} \phi'''' - \frac{(n^4 + 10n^2 \alpha^2 r^2 - 3\alpha^4 r^4)}{r^2 (n^2 + \alpha^2 r^2)^2} \phi'' \right. \\
& - \frac{2(n^2 + \alpha^2 r^2)}{r^2} \phi'' + \frac{2(n^2 + \alpha^2 r^2)}{r^3} \phi' + \frac{(n^6 + 3n^4 \alpha^2 r^2 + 23n^2 \alpha^4 r^4 - 3\alpha^6 r^6)}{r^2 (n^2 + \alpha^2 r^2)^2} \phi' \\
& \left. + \frac{(n^2 + \alpha^2 r^2)^2}{r^4} \phi - \frac{4n^2 (n^2 + 2\alpha^2 r^2)}{r^4 (n^2 + \alpha^2 r^2)} \phi - 2\alpha n \left(\Omega'' + \frac{(n^2 - \alpha^2 r^2) \Omega'}{(n^2 + \alpha^2 r^2) r} - \left(\alpha^2 + \frac{n^2}{r^2} \right) \Omega \right) \right\} \\
& = (U - c) \left\{ \phi'' + \frac{(n^2 - \alpha^2 r^2) \phi'}{(n^2 + \alpha^2 r^2) r} - \left(\alpha^2 + \frac{n^2}{r^2} \right) \phi \right\} - \phi \left\{ U'' + \frac{(n^2 - \alpha^2 r^2) U'}{(n^2 + \alpha^2 r^2) r} \right\} \quad 2-35
\end{aligned}$$

and

$$\begin{aligned}
& \frac{1}{i\alpha R} \left\{ \Omega'' + \frac{(n^2 + 3\alpha^2 r^2) \Omega'}{(n^2 + \alpha^2 r^2) r} - \left(\alpha^2 + \frac{n^2}{r^2} \right) \Omega + \frac{2\alpha n}{(n^2 + \alpha^2 r^2)^2} \left(\phi'' + \frac{(n^2 - \alpha^2 r^2) \phi'}{(n^2 + \alpha^2 r^2) r} \right. \right. \\
& \left. \left. - \left(\alpha^2 + \frac{n^2}{r^2} \right) \phi \right) \right\} = (U - c) \Omega - \frac{nU' \phi}{\alpha r (n^2 + \alpha^2 r^2)} \quad 2-36
\end{aligned}$$

with

$$\phi = -irv, \quad \Omega = (\alpha r w - nu) / (n^2 + \alpha^2 r^2) \quad 2-37$$

For the case of axisymmetric disturbances ($n=0$) and the disturbance equations (2-35) and (2-36) become uncoupled. Thus, equation (2-35) can be simplified and written as

$$\begin{aligned}
& \frac{1}{i\alpha R} \left(\phi'''' - \frac{2}{r} \phi'''' + \frac{3}{r^2} \phi'' - 2\alpha^2 \phi'' + \frac{2\alpha^2}{r} \phi' - \frac{3}{r^2} \phi' + \alpha^4 \phi \right) \\
& = (U - c) \left(\phi'' - \frac{1}{r} \phi' - \alpha^2 \phi \right) - \phi \left(U'' - \frac{U'}{r} \right) \quad 2-38
\end{aligned}$$

where

$$v^+ = \frac{i\phi}{r} e^{i\alpha(x-ct)} \quad 2-39$$

This disturbance equation for $n=0$ can be compared with that derived from the viewpoint of a stream function. The disturbances are related to the stream function ψ as

$$u^+ = \frac{1}{r} \frac{\partial \psi}{\partial r}, \quad v^+ = -\frac{1}{r} \frac{\partial \psi}{\partial x} \quad 2-40$$

where

$$\psi = \phi(r) e^{i\alpha(x-ct)} \quad 2-41$$

and $\phi(r)$ is the amplitude function. Substituting (2-41) into (2-40), one obtains

$$v^+ = -\frac{1}{r} i\alpha\phi(r) e^{i\alpha(x-ct)} \quad 2-42$$

Thus, the relationship between ϕ and ϕ is

$$\phi = -\alpha\phi \quad 2-43$$

This gives the perturbation equation for the axisymmetric disturbances in terms of the amplitude function as

$$\begin{aligned} \frac{1}{i\alpha R} \left\{ \phi'''' - \frac{2}{r} \phi'''' + \frac{3}{r^2} \phi'' - \frac{3}{r^3} \phi' + \alpha^2 \left(-2\phi'' + \frac{2}{r} \phi' + \alpha^2 \phi \right) \right\} \\ = (U-c) \left(\phi'' - \frac{1}{r} \phi' - \alpha^2 \phi \right) - \phi \left(U'' - \frac{U'}{r} \right) \end{aligned} \quad 2-44$$

Equation (2-44) can be directly derived from the two dimensional disturbance equations by using equations (2-40) and (2-41) and by eliminating the pressure terms.

Equations (2-35) through (2-44) are for azimuthally periodic disturbances and equation (2-44) is for the axisymmetric disturbances. All of these equations are

linear. The boundary conditions for these two different cases are discussed in the next section.

2. Boundary Conditions

The disturbances are subject to physical restrictions at the wall and at the center of the tube. These restrictions give rise to boundary conditions. For the case of azimuthally periodic disturbances, the boundary conditions to be satisfied by equations (2-31) through (2-34) at the wall are that the disturbance velocity components vanish due to viscosity and an impermeable tube wall.

$$u(1) = v(1) = w(1) = 0, \text{ for } n \neq 0 \quad 2-45$$

or

$$\phi(1) = \phi'(1) = \Omega(1) = 0, \text{ for } n \neq 0 \quad 2-46$$

The boundary conditions to be satisfied at the center of the tube, $r=0$, are that no fluid velocity or pressure be unbounded or discontinuous, that is, all disturbance quantities and their first order derivative must be finite. Since it is assumed that the velocity components and pressure vary as $\sin n\theta$ (or $\cos n\theta$), it is required that

$$u(0) = p(0) = 0, \text{ for } n \neq 0 \quad 2-47$$

Otherwise, u and p would be multi-valued at $r=0$. From the continuity equation (2-31) and equation (2-30), one also

has

$$v(0) = w(0) = 0, \quad n \neq 1 \quad 2-48$$

For $n=1$, the non-vanishing values of $v(0)$ and $w(0)$ are permissible (29), that is

$$v(0) + iw(0) = 0, \quad n=1 \quad 2-49$$

or

$$\phi(0) = \lim_{r \rightarrow 0} \{r^{2-n}\phi'(r)\} = \Omega(0) = 0, \quad n \neq 0 \quad 2-50$$

For the case of axisymmetric disturbances, $n=0$ and the conditions to be satisfied at the tube wall are

$$\phi(1) = \phi'(1) = 0, \quad n = 0 \quad 2-51$$

At the center of the tube, both u and p can have finite values

$$u(0) = \text{finite}, \quad p(0) = \text{finite}, \quad v(0) = 0, \quad n = 0 \quad 2-52$$

or from equations (2-40) and (2-41), one can write

$$\lim_{r \rightarrow 0} \frac{\phi}{r} = 0, \quad \lim_{r \rightarrow 0} \frac{\phi'}{r} = \text{finite} \quad 2-53$$

or

$$\phi(0) = 0, \quad \phi'(0) = 0 \quad 2-54$$

as will be seen later when the Frobenius series expansion is performed for $r \rightarrow 0$.

3. The Eigenvalue Problem

The coupled linear equations (2-35) and (2-36) with the boundary conditions (2-46) and (2-50) for the azimuthal disturbances constitute a homogeneous mathematical system. The same is true of the linear equation (2-44) along with the boundary conditions (2-51) and (2-54) for the axisymmetric disturbances. There exists, therefore, an eigenvalue problem for each in the form

$$E(\alpha, R, c, n) = 0 \quad 2-55$$

in which c is usually an eigenvalue which is to be sought for given values of α , R and n such that equation (2-55) is identically satisfied.

For the non-axisymmetric case with $n=1$, one integrates equations (2-35) and (2-36) from the center of the tube with the condition (2-50) toward the wall where the boundary condition (2-46) must be satisfied. Since the equations for ϕ and Ω are linear, the solutions for ϕ and Ω are expressible as

$$\begin{pmatrix} \phi \\ \phi' \\ \Omega \end{pmatrix} = \begin{pmatrix} \phi_1 & \phi_2 & \phi_3 \\ \phi_1' & \phi_2' & \phi_3' \\ \Omega_1 & \Omega_2 & \Omega_3 \end{pmatrix} \begin{pmatrix} a_1 \\ a_2 \\ a_3 \end{pmatrix} \quad 2-56$$

where ϕ_1 , ϕ_2 , ϕ_3 and Ω_1 , Ω_2 , Ω_3 are, respectively, the three independent solutions of ϕ and Ω . For a nontrivial solution which satisfies the conditions (2-46) at $r=1.0$ to exist, it is necessary that the determinant of the coefficient

matrix be zero at $r=1$, that is

$$\begin{vmatrix} \phi_1(1) & \phi_2(1) & \phi_3(1) \\ \phi_1'(1) & \phi_2'(1) & \phi_3'(1) \\ \Omega_1(1) & \Omega_2(1) & \Omega_3(1) \end{vmatrix} = 0 \quad 2-57$$

Similarly, for the case of axisymmetric disturbances ($n=0$), the equations corresponding to equations (2-56) and (2-57) are

$$\begin{pmatrix} \Phi \\ \Phi' \end{pmatrix} = \begin{pmatrix} \Phi_1 & \Phi_2 \\ \Phi_1' & \Phi_2' \end{pmatrix} \begin{pmatrix} a_1 \\ a_2 \end{pmatrix} \quad 2-58$$

and

$$\begin{vmatrix} \Phi(1) & \Phi(1) \\ \Phi_1'(1) & \Phi_2'(1) \end{vmatrix} = 0 \quad 2-59$$

Equation (2-57) or (2-59) is the so called secular equation and is, in general, a complex function of the parameters α , R , c and n . Mathematically, α is taken to be positive real, while c is allowed to be complex, that is, $c=c_r+ic_i$. The flow is unstable, neutrally stable, or stable, according to whether c_i is greater than, equal to, or less than zero.

The eigenvalue problem for both axisymmetric disturbances with $n=0$ and azimuthally periodic disturbances with $n=1$ are solved numerically. The numerical schemes employed in the solution are presented in the next chapter.

III. THE NUMERICAL METHODS OF SOLUTION

A. Introduction

In this chapter, the solutions of the linearized stability equations for axisymmetric and non-axisymmetric infinitesimal disturbances subject to their respective boundary conditions as mentioned in the previous chapter, will be discussed. Since the exact solutions to these equations are not known to exist, their solutions can only be obtained by approximate methods, such as an asymptotic solution, or by numerical methods. Recently, Gersting (30) made a systematic study of the numerical methods of solution for stability problems. These methods include the finite difference method (31,32,33), the variational method (34), and the numerical integration method (24,35,36,37). To remove the "parasitic errors" due to the numerical integration of the stability equations, Nachtsheim (35) used the matching technique while Kaplan (24) and Conte (36) employed the filtering and near-orthonormalization scheme, respectively. More recently, Davey and Nguyen (37) described a very simple "complete orthonormalization" procedure to solve the stability problem of Poiseuille pipe flow.

In this investigation, the filtering integration technique, the Gram-Schmidt orthonormalization procedure, and the complete orthonormalization procedure are examined. Even though the methods have been applied and described

by the previous investigators, a brief description of the numerical integration technique used in the present studies is given. The methods used to find the eigenvalues and to generate the neutral stability curves are also described.

The stability equations for pipe flow, equations (2-35), (2-36) and (2-44) have a regular singular point at the center of the pipe, $r=0$. Because of the singularity, a method has to be devised so that the integration can be started at $r=0$. This will be discussed first.

B. The Starting Value for Numerical Integration

To use the 4th-order Runge-Kutta integration scheme (37) for the solution of a mathematical system involving a differential equation of order n , the system must be transformed into an initial value problem in which the values of the function and its derivatives up to the $(n-1)$ th are initially specified. Since $r=0$ is a regular singular point of equation (2-35), (2-36) and (2-44), any self-starting integration methods have to be abandoned. Therefore, the Frobenius series solution is obtained and applied in the region $r>0$. The cases of axisymmetric and azimuthally periodic disturbances will be treated separately.

1. Axisymmetric Disturbances ($n=0$)

The solution of equation (2-44) near $r=0$ is assumed to have the form

$$\Phi = \sum_{i=0}^{\infty} c_i r^{\beta+i} \quad 3-1$$

In addition, the velocity profile based on the local maximum velocity in the entrance region is

$$U = \left\{ 2(1-r^2) + \sum_{i=1}^{\infty} \frac{4}{\alpha_i^2} \left(\frac{J_0(\alpha_i r)}{J_0(\alpha_i)} - 1 \right) e^{-\alpha_i^2 \chi} \right\} / \left\{ 2 + \sum_{i=1}^{\infty} \frac{4}{\alpha_i^2} \left(\frac{1}{J_0(\alpha_i)} - 1 \right) e^{-\alpha_i^2 \chi} \right\} \quad 3-2$$

Substituting (3-1) and (3-2) into equation (2-44) and putting the coefficient $c_0 \neq 0$, one finds $\beta=0, 2, 2, 4$. The double root, $\beta=2$, requires an additional $\log(r)$ term in the solution. Since the $\log(r)$ term is unbounded at $r=0$, and since $\beta=0$ cannot satisfy the boundary condition $\Phi(0)=0$, the single roots $\beta=2$ and $\beta=4$ are the only solution. It is very complicated to find the recursion formulas for c_i , but fortunately the series solutions require only the starting values at r near 0. From the two independent solutions corresponding, respectively, to $\beta=2$ and $\beta=4$

$$\Phi_1 = c_0 \{ r^2 + (-i\alpha R(A_1) - \alpha^4) r^6 / 192 + \dots \} \quad 3-3$$

and

$$\Phi_2 = c_2 \{ r^4 + (16\alpha^2 + 8i\alpha R(A_1)) r^6 / 192 + \dots \}$$

where $A_1 = 1 - c$

It can be seen that only one term is accurate enough for the initial value of integration from $r=10^{-4}$ or 10^{-5} . For simplicity a normalizing factor is applied such that the starting value at $r=0$ are defined as

$$\Phi_1(0) = \Phi_1'(0) = \Phi_1''(0) = 0, \quad \Phi_1'''(0) = 1.0 \quad 3-4$$

and

$$\Phi_2(0) = \Phi_2'(0) = \Phi_2''(0) = 0, \quad \Phi_2'''(0) = 1.0 \quad 3-5$$

After integrating to the tube wall where the boundary conditions (2-54) are applied, one can find the coefficients c_0 and c_1 , and the eigenvalue from the expression

$$\begin{pmatrix} \Phi_1(1) & \Phi_2(1) \\ \Phi_1'(1) & \Phi_2'(1) \end{pmatrix} \begin{pmatrix} c_1 \\ c_2 \end{pmatrix} = 0 \quad 3-6$$

in which c_0 and c_1 correspond to a_1 and a_2 in equation (2-58). The eigenvalue problem will be discussed later. Equation (3-4) and (3-5) give the starting value for the two independent solution Φ_1 and Φ_2 .

2. Non-Axisymmetric Disturbances with $n=1$

To solve the coupled equations (2-35) and (2-36), the series solutions are applied for $r \rightarrow 0$ as in the axisymmetric case. One starts by assuming the solutions for ϕ and Ω near $r=0$ in the form

$$\phi(r) = \sum_{i=0}^{\infty} c_i r^{\beta+i} \quad 3-7$$

and

$$\Omega(r) = \sum_{m=0}^{\infty} d_m r^{\gamma+m} \quad 3-8$$

After expanding the coefficients of the coupled equations (2-35) and (2-36) into power series by the binomial theory and substituting (3-7) and (3-8) into these equations, one obtains the series solutions for ϕ and Ω as

$$\begin{aligned}\phi(r) = & c_0 \{r - (13\alpha^4 + 3i\alpha^3 RA_1)r^5/192 + \dots\} \\ & + c_2 \{r^3 + (48\alpha^2 + 8i\alpha RA_1)r^5/192 + \dots\} \\ & + d_0 \{(-8\alpha^3 + 2i\alpha^2 RA_1)r^5/192 + \dots\}\end{aligned}\quad 3-9$$

and

$$\begin{aligned}\Omega(r) = & c_0 \{(6\alpha^3 - iRB_1)r^3/8 + \dots\} \\ & + c_2 \{-2\alpha r^3 + \dots\} \\ & + d_0 \{r - (\alpha^2 - i\alpha RA_1)r^3/8 + \dots\}\end{aligned}\quad 3-10$$

where

$$A_1 = 1 - c$$

$$B_1 = \left\{4 + \sum_{i=1}^{\infty} \frac{2}{J_0(\alpha_i)} e^{-\alpha_i^2 \chi}\right\} / \left\{2 + \sum_{i=1}^{\infty} \frac{4}{\alpha_i^2} \left(\frac{1}{J_0(\alpha_i)} - 1\right) e^{-\alpha_i^2 \chi}\right\}$$

and c_0 , c_2 and d_0 are the undetermined coefficients. For simplicity, a scaling factor is applied. The starting value for the three independent solutions at $r=0$ are

$$\phi_1 = \phi_1'' = \phi_1''' = \Omega_1 = \Omega_1' = 0, \quad \phi_1' = 1.0 \quad 3-11$$

$$\phi_2 = \phi_2' = \phi_2'' = \Omega_2 = \Omega_2' = 0, \quad \phi_2''' = 1.0 \quad 3-12$$

and

$$\phi_3 = \phi_3' = \phi_3'' = \phi_3''' = \Omega_3 = 0, \Omega_3' = 1.0 \quad 3-13$$

By integrating to the tube wall and applying the boundary conditions (2-46), one can calculate the eigenvalue and the coefficients c_0 , c_2 and d_0 from

$$\begin{pmatrix} \phi(1) \\ \phi'(1) \\ \Omega(1) \end{pmatrix} = \begin{pmatrix} \phi_1(1) & \phi_2(1) & \phi_3(1) \\ \phi_1'(1) & \phi_2'(1) & \phi_3'(1) \\ \Omega_1(1) & \Omega_2(1) & \Omega_3(1) \end{pmatrix} \begin{pmatrix} c_0 \\ c_2 \\ d_0 \end{pmatrix} \quad 3-14$$

where c_0 , c_2 , d_0 correspond, respectively, to a_1 , a_2 , a_3 in equation (2-56). The solution of the eigenvalue problem is discussed in section III-D.

C. The Numerical Integration Schemes

The 4th-order Runge-Kutta scheme is used for the direct integration of the stability equations from near the center of the tube ($r \rightarrow 0$) to the tube wall. It is well known that instability of duct flows occurs at large Reynolds numbers. Thus, during the numerical integration, one of the two independent solutions for the 4th-order problem described by equation (2-44) and at least one of the three independent solutions for the 6th-order problem described by equations (2-35) and (2-36) grows very rapidly. These inherent "parasitic errors" cause the independent solutions to lose their characteristics and become dependent. It is, therefore, difficult to deal with these kinds of

stability equations for large Reynolds numbers. There are various methods which are employed to reduce or remove the so-called "parasitic errors" and thus maintain the solutions independent during the integration. Three of these methods are described below.

1. The Filtering Technique

Kaplan (24) presented a purification scheme for controlling the parasitic errors during the integration of the stability equation. For example, let ϕ_g be the rapidly growing solution and ϕ_s be the slowly growing solution for the case of axisymmetric disturbances. The mesh point in the region $0 \leq r \leq 1$ are $i=0,1,2,3,\dots,n$. It is not necessary to remove the parasitic errors totally, but merely to insure that ϕ_g does not dominate the slowly growing solution ϕ_s at each step of the calculation. Kaplan suggested that this could be done by introducing a linear operator F which has the following properties: (1) $F\{\phi_g(i)\}$ is not zero at any mesh point i ; (2) the auxiliary differential equation $F(\phi)=0$ has a solution that always behaves much differently from the rapidly growing solution ϕ_g in that it does not have such a rapid growth; and (3) the operator F keeps the order of magnitude of its argument. Then the slowly growing solution ϕ_s can be purified by the equation,

$$\tilde{\phi}_s(i) = \bar{\phi}_s(i) - \frac{F\{\bar{\phi}_s(i)\}}{F\{\phi_g(i)\}}\phi_g(i) \quad 3-15$$

at every step of the numerical integration. In this equation, $\tilde{\phi}_s$ is the purified, behaved solution and $\bar{\phi}_s$ is the calculated slowly growing solution before purification. A detailed account of this technique is given by Gersting (30).

This technique is applied to the two problems of interest in the present study. The terms on the right-hand side of equations (2-35), (2-36) and (2-44) represent the inviscid part and those on the left-hand side represent the viscous part. The inviscid part of the stability equations (2-35) and (2-44) is used as the auxiliary operator F, namely,

$$\text{Filter} = \frac{F(\text{slowly growing solution})}{F(\text{rapidly growing solution})} \quad 3-16$$

where for $n \neq 0$

$$F(\phi)_m = \left\{ (U-c) \left(\phi'' + \frac{(n^2 - \alpha^2 r^2)}{r(n^2 + \alpha^2 r^2)} \phi' - \left(\alpha^2 + \frac{n^2}{r^2} \right) \phi \right) - \phi \left(U'' + \frac{(n^2 - \alpha^2 r^2)}{r(n^2 + \alpha^2 r^2)} U' \right) \right\}, \quad m=1,2,3 \quad 3-17$$

and for $n=0$

$$F(\phi)_m = \left\{ (U-c) \left(\phi'' - \frac{1}{r} \phi' - \alpha^2 \phi \right) - \phi \left(U'' - \frac{U'}{r} \right) \right\}, \quad m=1,2 \quad 3-18$$

The three conditions on the operator F are now

examined. (1) $F(\phi_g)$ is not zero, since ϕ_g is a viscous solution and will not satisfy the inviscid solution. (2) The solution $F(\phi)=0$ is an inviscid solution which does not grow rapidly and behaves differently from ϕ_g . (3) F preserves the order of magnitude in that $F(\bar{\phi}_s)$ is smaller because $\bar{\phi}_s$ is an inviscid-like solution and for an exact inviscid solution $F(\phi_{\text{inviscid}})=0$, and that $F(\phi_g)$ is larger since ϕ_g is a viscous-like solution and is not annihilated by the inviscid operator. This shows that equations (3-17) and (3-18) can be the auxiliary operators which accompany equation (3-15). This completes the presentation of Kaplan's filtering method.

For non-axisymmetric infinitesimal disturbances, the scheme consists of extracting from solution two and solution three a portion of the fastest growing solution (solution one) and then extracting from solution three a portion of the intermediate growing solution (solution two). For large values of αR , overflow occurred in an IBM 360/50 computer during the integration, since complex number operation was needed. Thus, the filtering scheme was not used for very large values of αR in the present integration.

2. Gram-Schmidt Orthonormalization Procedure

Wazzan, Okamura, and Smith (25) replaced the Kaplan's purification scheme by the Gram-Schmidt Orthonormalization

procedure to insure that the solutions are linearly independent. Because of the round-off, Φ_S has a small parasitic error which is proportional to Φ_g . To remove this parasitic error from the integration solution, an auxiliary solution $\bar{\Phi}_S$ is introduced such that no component of Φ_S is contained in it. This can be done by normalizing the integrated values of Φ_g at the end of each step of the integration. The normalized values are denoted by $\bar{\Phi}_g$. At each sub-interval i , let

$$\bar{\Phi}_S(i) = \Phi_S(i) - A\bar{\Phi}_g(i) \quad 3-19$$

Since it is desired to remove any presence of the solution Φ_g from $\bar{\Phi}_S$, $\bar{\Phi}_S$ is constructed to be orthogonal to $\bar{\Phi}_g$.

Hence

$$A = \langle \Phi_S(i), \bar{\Phi}_g(i) \rangle \quad 3-20$$

and

$$\bar{\Phi}_S(i) = \Phi_S(i) - \langle \Phi_S(i), \bar{\Phi}_g(i) \rangle \bar{\Phi}_g(i) \quad 3-21$$

That is

$$\bar{\Phi}_S(i) = \Phi_S(i) - \frac{\langle \Phi_S(i), \bar{\Phi}_g(i) \rangle}{\langle \bar{\Phi}_g(i), \bar{\Phi}_g(i) \rangle} \bar{\Phi}_g(i) \quad 3-22$$

in which the notation \langle , \rangle denotes the inner product, whereas

Φ is the functional space containing $(\Phi_j, \Phi_j', \Phi_j'', \Phi_j''')$ with $j=1,2$, for $n=0$ or $(\phi_j, \phi_j', \phi_j'', \phi_j''', \Omega_j, \Omega_j')$ with $j=1,2,3$, for $n \neq 0$.

The procedure is very similar to the filtering technique. The advantage of this method is that after each step of the integration, the functional space can be normalized to avoid the overflow limit of the computer. As mentioned before, it is not necessary to remove the parasitic error totally, but merely to insure that the Φ_g does not dominate the slowly growing solution Φ_s at each step of the calculation. Conte (36) presented the near-orthonormalization technique by setting a criterion to perform the orthonormalization when necessary, instead of performing orthonormalization at every mesh point.

3. "Complete" Orthonormalization

This technique was proposed recently by Davey and Nguyen (37). Suppose that $F(\Phi)=0$, where F is a fourth-order operator, has the range of integration $0 \leq r \leq 1$ and has two boundary conditions on Φ at each end. Let $y = \{\Phi, \Phi', \Phi'', \Phi'''\}$ and choose n steps of mesh size h for the region $0 \leq r \leq 1$. If a condition $y = y_i$ is given when $r = ih$ and if one integrates to obtain $y = y_{i+1}$ at $r = (i+1)h$, the relationship between y_i and y_{i+1} can be expressed as $y_{i+1} = A^i y_i$, where A^i is a 4×4 matrix whose elements will be independent of y_i . By letting y_i have the value

$\{0,0,0,1\}$, $\{0,0,1,0\}$, $\{0,1,0,0\}$ and $\{1,0,0,0\}$ in turn, one may readily determine A^i . This process is repeated for each subinterval to find $A^0, A^1, A^2, \dots, A^{n-1}$.

The relationship between y_0 and y_n will be of the form

$$y_n = B y_0 \quad 3-23$$

with the matrix

$$B = A^{n-1} \dots A^0 \quad 3-24$$

An iteration technique may be used to find the eigenvalues from $y_0 = B^{-1} y_n$ along with the boundary conditions. This technique was proposed by Davey and Nguyen (37) to improve the filtering technique of Kaplan (24) in their study of the stability of Poiseuille pipe flow.

The numerical results of the eigenvalues $c = c_r + ic_i$ from the various integration techniques discussed above will be presented and compared in chapter IV.

D. Iteration Procedure for Determining the Eigenvalues

The initial value technique to solve the eigenvalue problem (equation (2-55)) leads to the requirement that an iteration procedure be employed to determine the eigenvalues. Two different techniques, Muller's method and the differential-correction method, are used along with the Runge-Kutta numerical integration scheme to obtain the

eigenvalues and points on the neutral stability curves.

For the case of $n=1$, integration from the tube center to the tube wall gives at $r=1$

$$a_1 \phi_1(1) + a_2 \phi_2(1) + a_3 \phi_3(1) = \phi(1) = 0 \quad 3-25$$

$$a_1 \phi_1'(1) + a_2 \phi_2'(1) + a_3 \phi_3'(1) = \phi'(1) = 0 \quad 3-26$$

$$a_1 \Omega_1(1) + a_2 \Omega_2(1) + a_3 \Omega_3(1) = \Omega(1) = 0 \quad 3-27$$

$$a_1 \phi_1''(1) + a_2 \phi_2''(1) + a_3 \phi_3''(1) = \phi''(1) = 1.0 \quad 3-28$$

Similarly, for the axisymmetric case with $n=0$, one obtains

$$a_1 \Phi_1(1) + a_2 \Phi_2(1) = \Phi(1) = 0 \quad 3-29$$

$$a_1 \Phi_1'(1) + a_2 \Phi_2'(1) = \Phi'(1) = 0 \quad 3-30$$

$$a_1 \Phi_1''(1) + a_2 \Phi_2''(1) = \Phi''(1) = 1.0 \quad 3-31$$

There are two approaches which can be used to find the coefficient a_i and the eigenvalues. For instance, consider the case of $n=1$: (1) For a non-trivial solution from the boundary conditions (3-25) through (3-27), an iteration technique is applied to find the eigenvalues which satisfies the condition that the determinant of the coefficient matrix a_i be zero. Next, one assigns $a_3=(1.0,0.0)$ to find a_1 and a_2 from any of the two equations. (2) In addition to the boundary conditions (3-25) through (3-27), one more equation (3-28) is used. Since there is no specific boundary condition for $\phi''(1)$, the choice for

$\phi''(1)=1$ is arbitrary. As long as $\phi''(1)$ is non-zero, the value assumed merely changes the normalization factor for ϕ . By solving equations (3-26) through (3-28) for the a_i and using equation (3-25) as the test function, one can find the eigenvalues by iteration. In this method, the coefficients a_i and the eigenvalues are found at the same time when all the boundary conditions are satisfied.

There are three case which can be considered in solving the equation $E(\alpha, R, n, c) = 0$ in the eigenvalue problem: (1) For given values of n , α and R , the eigenvalue $c = c_r + c_i$ is found by an iteration technique. (2) To find a point (α, R) on the neutral stability curve, the values of n , α and $c_i = 0$ are given and the values of R and c_r are sought by iteration. Or (3) One can give the values of n , R and $c_i = 0$ and obtain the values of α and c_r for a point on the neutral stability curve, again by an iteration procedure.

One of the two iteration techniques used in this investigation is Muller's method (39). It is an iterative procedure for finding the real and complex roots of a polynomial equation $G(x) = 0$ whose coefficient may be complex. This procedure selects three arbitrary points x_1 , x_2 and x_3 as the starting values. The next approximation to the root, x_4 , is taken to be one of the zeros of the second degree polynomial which passes through the functional values $G(x_1)$, $G(x_2)$ and $G(x_3)$. The iterative procedure

is continued by dropping the first point and considering the second point as the first point, the third point as the second point and the fourth point as the third point. The advantages of this method are: (1) the complex roots can be obtained; (2) the iteration requires only the evaluation of the functional value and does not include the value of the derivatives of the function; and (3) after the three initial estimates have been processed, only a single pass through the integration procedure is required for each iteration. This procedure is used to obtain the eigenvalues for given values of α , R and n . A second iteration scheme was used in obtaining points on the neutral stability curve with $c_i=0$. This is described in the following section.

E. Generation of the Neutral Stability Curve

The differential-correction method is used for locating point on the neutral stability curves. This method is based on the representation of the expression for an exact differential by a difference equation. If $G=G_r+iG_i$ is a function of the variables x_1 and x_2 , then

$$dG = \frac{\partial G}{\partial x_1} dx_1 + \frac{\partial G}{\partial x_2} dx_2 \quad 3-32$$

That is,

$$dG_r = \frac{\partial G_r}{\partial x_1} dx_1 + \frac{\partial G_r}{\partial x_2} dx_2 \quad 3-33$$

and

$$dG_i = \frac{\partial G_i}{\partial x_1} dx_1 + \frac{\partial G_i}{\partial x_2} dx_2 \quad 3-34$$

If the difference operator Δ is applied, one obtains

$$\Delta G_r = \left. \frac{\Delta G_r}{\Delta x_1} \right|_{x_2} \Delta x_1 + \left. \frac{\Delta G_r}{\Delta x_2} \right|_{x_1} \Delta x_2 \quad 3-35$$

and

$$\Delta G_i = \left. \frac{\Delta G_i}{\Delta x_1} \right|_{x_2} \Delta x_1 + \left. \frac{\Delta G_i}{\Delta x_2} \right|_{x_1} \Delta x_2 \quad 3-36$$

Suppose that ξ_1 and ξ_2 are the eigenvalues which satisfy $G(\xi_1, \xi_2) = 0$. Let x_1 and x_2 be the first estimate for the eigenvalues such that $G(x_1, x_2) \neq 0$. The difference equations (3-35) and (3-36) are then used to find Δx_1 and Δx_2 . The next estimates for the eigenvalues are taken to be $x_1 + \Delta x_1$ and $x_2 + \Delta x_2$ which will make $G(x_1 + \Delta x_1, x_2 + \Delta x_2)$ closer to zero, and so on. The final estimates which give $G = 0$ are the desired eigenvalues ξ_1 and ξ_2 . In the present problem, $G = E(\alpha, n, c_r, c_i) = 0$. For the given three parameters, say $\alpha, n, c_i = 0$, the other two parameters R and c_r are to be found. This is done as follows. For given values of α, n and $c_i = 0$:

- (1) Select $x_1 = R, x_2 = c_r$ and find ΔG .
- (2) Select $x_1 = R + \Delta R, x_2 = c_r$ and find $\frac{\Delta G}{\Delta x_1}$
- (3) Select $x_1 = R, x_2 = c_r + \Delta c_r$ and find $\frac{\Delta G}{\Delta x_2}$

(4) Find Δx_1 and Δx_2 from the equation

(5) The new estimates for x_1 and x_2 are then

$$x_{1\text{new}} = x_1 + \Delta x_1$$

$$x_{2\text{new}} = x_2 + \Delta x_2$$

The above procedure is repeated until G approaches zero. The disadvantage of this procedure is that it requires three passes through the integration for each iteration. However, if the initial estimate is close to the actual eigenvalue the disadvantage is offset by the fact that it gives the partial derivative which is used in the iteration with a more rapid convergence for the iteration.

The neutral stability curve for a given n is generated as follows. Suppose that a point (α, R) is found on the neutral curve ($c_i=0$) as described above. One can increase or decrease α , using R and c_r from the previous point as the initial estimates to find the new values of R and c_r for which $c_i=0$, and so on. In this way, the neutral stability curve can be systematically mapped out. One can also find α and c_r for given n , R and $c_i=0$. This latter approach is useful in mapping that portion of the neutral stability curve, such as the upper branch of the curve, where the change in α with respect to R is rather slow.

The numerical results for the eigenvalues, the neutral stability curves and the critical Reynolds numbers for

various axial locations in the entrance region of the pipe are presented and discussed in Chapter IV.

F. Calculation of Eigenfunctions

Once the eigenvalue is available, the eigenfunction can be found easily by the Gram-Schmidt orthonormalization procedure. In the orthonormalization technique, one divides the region $0 \leq r \leq 1$ into n equal sub-divisions of mesh size h so that $r_i = ih$ where $i = 1, 2, \dots, n$. The base solution $Q(r_i) = (q_i^{(1)}, \dots, q_i^{(k)})$ can be obtained by applying any standard integration method. The Gram-Schmidt procedure is then used to orthonormalize the base solution. At mesh point i , the matrix of the base solutions $Q(r_i)$ is orthonormalized by multiplying with a $k \times k$ matrix $P^{(i)}$, such that

$$Z(r_i) = Q(r_i)P^{(i)} \quad 3-37$$

If the vectors in $Q(r_i)$ are linearly independent, it is always possible to find such a matrix $P^{(i)}$. Moreover, $P^{(i)}$ is a nonsingular upper triangular matrix

$$P^{(i)} = \begin{pmatrix} P_{11} & P_{12} & \cdot & \cdot & \cdot & P_{1k} \\ 0 & P_{22} & \cdot & \cdot & \cdot & P_{2k} \\ 0 & \cdot & \cdot & \cdot & \cdot & \cdot \\ 0 & \cdot & \cdot & \cdot & \cdot & P_{kk} \end{pmatrix} \quad 3-38$$

For a given $n \times k$ matrix $Q(r_i)$, one can obtain the element P_{ij} of $P^{(i)}$ as follows: Let a set of vector $(q_i^{(1)}, \dots, q_i^{(k)})$

the eigenvalue and the coefficients $\beta^{(n)}$ are obtained by satisfying the boundary conditions such as described previously in section III-D.

The function $y(r_i)$ at all mesh points except the end point $i=n$ is obtained by backward transformation in the following manner. At the end point r_n , combination of equations (3-41) and (3-42) gives

$$y(r_n) = Z(r_n) \beta^{(n)} = Q(r_n) \beta^{(n-1)} \quad 3-43$$

where $\beta^{(n-1)} = p^{(n)} \beta^{(n)}$. Then, at the point r_{n-1} , one has

$$y(r_{n-1}) = Z(r_{n-1}) \beta^{(n-1)} = Q(r_{n-1}) \beta^{(n-2)} \quad 3-44$$

where $\beta^{(n-2)} = p^{(n-1)} \beta^{(n-1)}$, and so on. Thus, the function $y(r_i)$ at any point r_i is expressible as

$$y(r_i) = Q(r_i) \beta^{(i-1)}, \quad i = n, n-1, \dots, 1 \quad 3-45$$

with $\beta^{(i-1)} = p^{(i)} \beta^{(i)}$. Since $Q(r_i)$ or $Z(r_i)$ and $p^{(i)}$ are known from the eigenvalue calculation, and since $\beta^{(i-1)}$ is related to the known value of $\beta^{(i)}$ one step ahead, $y(r_i)$ can be computed from equation (3-45).

In terms of the notations used for the case of $n = 1$, equation (3-45) as applied at any point $0 \leq r \leq 1$ has the form

$$\begin{pmatrix} \phi \\ \phi' \\ \phi'' \\ \phi''' \\ \Omega \\ \Omega' \end{pmatrix} = \begin{pmatrix} \phi_1 & \phi_2 & \phi_3 \\ \phi'_1 & \phi'_2 & \phi'_3 \\ \phi''_1 & \phi''_2 & \phi''_3 \\ \phi'''_1 & \phi'''_2 & \phi'''_3 \\ \Omega_1 & \Omega_2 & \Omega_3 \\ \Omega'_1 & \Omega'_2 & \Omega'_3 \end{pmatrix} \begin{pmatrix} \beta_1 \\ \beta_2 \\ \beta_3 \end{pmatrix} \quad 3-46$$

wherein the β_i ($i = 1, 2, 3$) vary from point to point.

Similarly, for the case of $n = 0$, it can be written as

$$\begin{pmatrix} \Phi \\ \Phi' \\ \Phi'' \\ \Phi''' \end{pmatrix} = \begin{pmatrix} \Phi_1 & \Phi_2 \\ \Phi'_1 & \Phi'_2 \\ \Phi''_1 & \Phi''_2 \\ \Phi'''_1 & \Phi'''_2 \end{pmatrix} \begin{pmatrix} \beta_1 \\ \beta_2 \end{pmatrix} \quad 3-47$$

The eigenfunctions ϕ , ϕ' , Ω and Φ , Φ' are computed, respectively, for the cases $n = 1$ and $n = 0$. Their results are presented in the following Chapter.

IV. RESULTS AND DISCUSSION

In the preceding chapters, the eigenvalue problems and the methods to find the eigenvalues and the neutral stability curves are discussed in sufficient detail. The main flow velocity solution U and its first and second derivative with respect to r are evaluated from equation (2-10). With these main flow quantities available, the stability problem can be handled. The stability results were obtained for the least stable wall mode, as was explained in the introduction.

The numerical results are obtained with an IBM 360/50 digital computer. They are presented and discussed in this chapter.

A. The Eigenvalues

The eigenvalue problem is described by equation (2-55), namely,

$$E(\alpha, R, n, c) = 0$$

The numerical integration schemes used to solve for the eigenvalues were discussed in Section D, chapter III. To obtain an eigenvalue c for given values of α and R by Muller's iteration technique, one needs to have three c values to get started. One guesses an eigenvalue c and may take the other two as $(1 \pm 0.02)c$. When these three c

values are guessed close to the actual eigenvalue, only a few iterations are required for a convergence. The eigenvalues c for the Poiseuille pipe flow are available for both axisymmetric disturbances (15) and non-axisymmetric disturbances (17,40).

For the case of axisymmetric disturbances $n=0$, the eigenvalues for given values of α and R at various axial locations in the entrance region were obtained as follows. The eigenvalue $c=0.3536-i0.0954$ for $\alpha=1.0$ and $R=5000$ as given by Davey and Drazin (15) for the fully developed flow was reproduced and used along with two other values, $(1\pm 0.02)c$, as the initial guessed values for the location $\chi=0.2$ and for the same α , R values. When the eigenvalue at $\chi=0.2$ is obtained, one uses it as the initial guessed eigenvalue to determine the eigenvalue for the next χ with the same α and R , and so on, until $\chi=0.002$. With c known for each χ , the neutral stability curve at each χ can be generated. In Table 3, the eigenvalues for $\alpha=1.0$, $R=5000$, $n=0$ with $N=100$ steps over $0\leq r\leq 1$ are shown for different axial locations. The results are from double precision arithmetic computation.

It can be seen from Table 3 that the filter method and the complete orthonormalization method give eigenvalues which agree well at different χ values. The general Runge-Kutta integration scheme without any purification failed when χ is smaller than 0.04. Moreover, the results

at $\chi=0.05$ and 0.06 do not agree well with those obtained with the purification technique. The complete orthonormalization method of Davey and Nguyen (37) failed when χ reached 0.01 . From Table 3, one can see the advantage of using the Kaplan filter technique. However, this scheme causes overflow in an IBM 360/50 computer when αR is very large. In this study, the Gram-Schmidt procedure was used as a supplement to Kaplan's technique.

The eigenvalues c for non-axisymmetric small disturbances with $n=1$ were calculated for the fully developed flow. The results from both single and double precision arithmetic operations for $\alpha=1.0$ and $R=6000$ are listed in Table 4. They agree with those given in reference (39). The single precision gives results which are as good as those from double precision calculations.

The eigenvalues at various axial locations for the non-axisymmetric case were obtained in a manner similar to that described for the axisymmetric case. A comparison of the eigenvalues at $\chi=0.006$ with $\alpha=1.9$ and $R=23800$ is made in Table 5 for various purification schemes. As in the case of fully developed flow, Table 4, the single precision operation gives accurate results. Thus, the single precision arithmetic operation was used in the numerical calculations.

Table 3

A Comparison of Eigenvalues c Obtained
with Various Techniques, $n=0$, $\alpha=1.0$, $R=5000$, $N=100$

χ	Filter	Orthonormalization	No Purification
	c	c	c
∞		0.35496-i0.09543	0.35356-i0.09544
0.2	0.35496-i0.09538	0.35496-i0.09538	
0.1	0.37364-i0.09427	0.37364-i0.09427	0.35748-i0.09632
0.08	0.38835-i0.09284	0.38835-i0.09284	0.36505-i0.09186
0.07	0.39948-i0.09129	0.39948-i0.09129	
0.06	0.41420-i0.08842	0.41420-i0.08842	0.39092-i0.08281
0.05	0.43319-i0.08282	0.43319-i0.08283	0.38818-i0.09292
0.04	0.45564-i0.07198	0.45563-i0.07194	
0.03	0.47603-i0.05453	0.47603-i0.05463	
0.02	0.48526-i0.03903	0.48546-i0.03890	
0.015	0.48365-i0.03980	0.48156-i0.04007	
0.010	0.47613-i0.05647		
0.009	0.47353-i0.06328		
0.008	0.47038-i0.07184		
0.007	0.46660-i0.08256		
0.006	0.46213-i0.09594		
0.005	0.45716-i0.11279		
0.004	0.45247-i0.13453		
0.003	0.45049-i0.16445		
0.002	0.45915-i0.21181		

Table 4

A Comparison of Eigenvalues for the Fully Developed Flow

 $n=1.0$, $N=100$

	$\alpha=1.0$, $R=6000$		$\alpha=0.98$, $R=2200$	
	c_r	c_i	c_r	c_i
Liu (40)	0.313	-i0.0521	0.398318	-i0.067752
Filter Single precision	0.313291	-i0.052140	0.398351	-i0.067829
Filter Double precision	0.313291	-i0.052141	0.398348	-i0.067832
Orthonormalization Single precision	0.313292	-i0.052141	0.398349	-i0.067832
Orthonormalization Double precision	0.313291	-i0.052141	0.398348	-i0.067832

Table 5

A Comparison of Eigenvalues for the Developing Flow at

 $\chi=0.006$, $\alpha=1.9$, $R=23800$, $n=1.0$ and $N=150$

	c_r	c_i
Filter Single precision	0.325959	-i0.001373
Filter Double precision	0.325957	-i0.001373
Orthonormalization Single precision	0.325958	-i0.001374
Orthonormalization Double precision	0.326198	-i0.001310

B. The Effect of Stepsize on the Accuracy of Eigenvalues

For the numerical results to be accurate, the number of steps required in the numerical integration needs to be checked. In Table 6 are shown the variations of the eigenvalues (c_r, R) or (c_r, c_i) for given values of $(\alpha, c_i=0)$ or (α, R) with the number of steps used in the integration. The actual number of steps used in the stability calculations at different entrance locations are listed in Table 7. It is seen from Table 7 that as χ becomes smaller, that is, as the entrance is approached, a smaller stepsize required for accurate numerical results, because the main flow velocity solution at a smaller χ value has a more rapid change near the tube wall.

C. The Neutral Stability Curves

By knowing an eigenvalue c for given values of α , R and n at a certain axial location χ , the points on the neutral stability curve can be obtained. This is done as follows. At a fixed χ , one increases R or α and checks the change of c_i (with respect to its sign) to judge the stability characteristics. For instance, for the axisymmetric case with $\chi=0.005$, the Reynolds number R was increased from 5000 to 30,000 and the wave number α was increased from 1.0 to 2.5. The variations of the eigenvalue with α and R are listed in Table 8. Inspection of Table 8 shows that for $\alpha=2.5$, a Reynolds number for neutral

Table 6

The Effect of Number of Steps on the Accuracy of Eigenvalues

χ	N	R	α	c_r	c_i	n
0.002	100	38962	3.5	0.316189	0	0
0.002	200	36573	3.5	0.321617	0	0
0.002	250	36547	3.5	0.321743	0	0
0.005	150	25000	2.5	0.340756	-0.000069	0
0.005	200	25000	2.5	0.340841	-0.000044	0
0.006	150	24063	1.8	0.346621	0	0
0.006	200	24051	1.8	0.346699	0	0
0.006	150	23781	1.9	0.346434	0	0
0.006	200	23763	1.9	0.346528	0	0
0.006	150	23881	2.0	0.345479	0	0
0.006	200	23832	2.0	0.345640	0	0
0.010	100	45000	0.8	0.343068	0.000169	0
0.010	150	45000	0.8	0.343230	0.000238	0
0.007	150	24360	1.9	0.324897	0	1.0
0.007	200	24317	1.9	0.325027	0	1.0
0.009	150	24686	1.6	0.318267	0	1.0
0.009	200	24667	1.6	0.318337	0	1.0
0.010	100	29928	1.2	0.299456	0	1.0
0.010	150	29842	1.2	0.299711	0	1.0

Table 7
 Number of Steps Used in the Calculations
 at Various Axial Locations

χ	N	χ	N
0.002	200	0.008	150
0.003	200	0.009	150
0.005	150	0.010	100
0.006	150	0.015	100
0.007	150		

Table 8
 Variation of Eigenvalues $c=c_r+c_i$ with α and R ($n=0$, $\chi=0.005$)

N	R	α	c_r	c_i
100	5000	1.0	0.457161	-0.112790
100	8000	1.0	0.426084	-0.078168
100	10000	1.0	0.412333	-0.063782
100	10000	1.2	0.405990	-0.052270
100	10000	1.4	0.401717	-0.043206
100	10000	1.6	0.398898	-0.035969
100	10000	1.8	0.397130	-0.030182
100	10000	2.0	0.396127	-0.025596
100	10000	2.5	0.395690	-0.018317
150	20000	2.5	0.353582	-0.002604
150	25000	2.5	0.340756	-0.000069
150	30000	2.5	0.330566	0.001163

stability ($c_i=0$) exists somewhere between 25,000 and 30,000. The differential-correction technique was then applied to locate the neutral point. It was found that $R=25,199$ and $c_r=0.340308$ for $\alpha=2.5$ and $c_i=0$. Once a neutral point is found, the next neutral point adjacent to it can be found by either changing the wave number α or the Reynolds number R and using the eigenvalue from the previous point as the initial guessed value to find the new set of eigenvalues R and c_r or α and c_r for which $c_i=0$, and so on. By proceeding in this fashion, the points (α,R) for $c_i=0$ are obtained and the neutral stability curve is generated.

There are two approaches which can be used with advantage in generating the neutral stability curve. To calculate the points on the lower branch of the neutral stability curve, one fixes α and $c_i=0$ to find the corresponding R and c_r . To obtain a point on the upper branch of the neutral stability curve, one fixes R and $c_i=0$ to find the corresponding α and c_r . This approach is effective in mapping out a neutral stability curve with a minimum amount of computer time.

1. The Neutral Stability Curves for Axisymmetric Disturbances

The neutral stability results for axisymmetric disturbances were obtained for axial locations $\chi=0.010$, 0.009, 0.006, 0.003 and 0.002. The computer outputs are

tabulated in Table B-1 through B-7, Appendix B, and are plotted in Figure 2. In the plot, $R^* = r_0^* \bar{u}^* / \nu$ is used as the abscissa instead of $R = r_0^* u_{\max}^* / \nu$. This is because the R^* value is based on the average velocity of the flow which is constant, whereas R is a local quantity and varies with axial locations χ , since the maximum velocity u_{\max}^* depends on χ . The relationship between X and χ is given in Figure 1 and in Table A-1, Appendix A. It is seen from the figure that the flow becomes more and more unstable as the axial distance χ increases from zero at the inlet, becomes the least stable at some distance χ , and then becomes more and more stable as χ increases farther downstream. Finally, the flow becomes absolutely stable in the fully developed region.

Figure 2 also indicates that the flow is unstable at a larger wave number α when χ is smaller. As χ increases, on the other hand, the instability of flow occurs at a lower α value. For a fixed axial location, the unstable region encompasses a larger range of α when χ is smaller.

The variation of the critical Reynolds number R^* with tube axial position is illustrated in Figure 3. The data for the curve are tabulated in Table D-1, Appendix D. An inspection of Figure 3 reveals that as the axial distance increases, the critical Reynolds number decreases, reaches the minimum value of about 19900 at $X=0.00325$ (i.e., $\chi=0.00629$) and then increases monotonically with distance

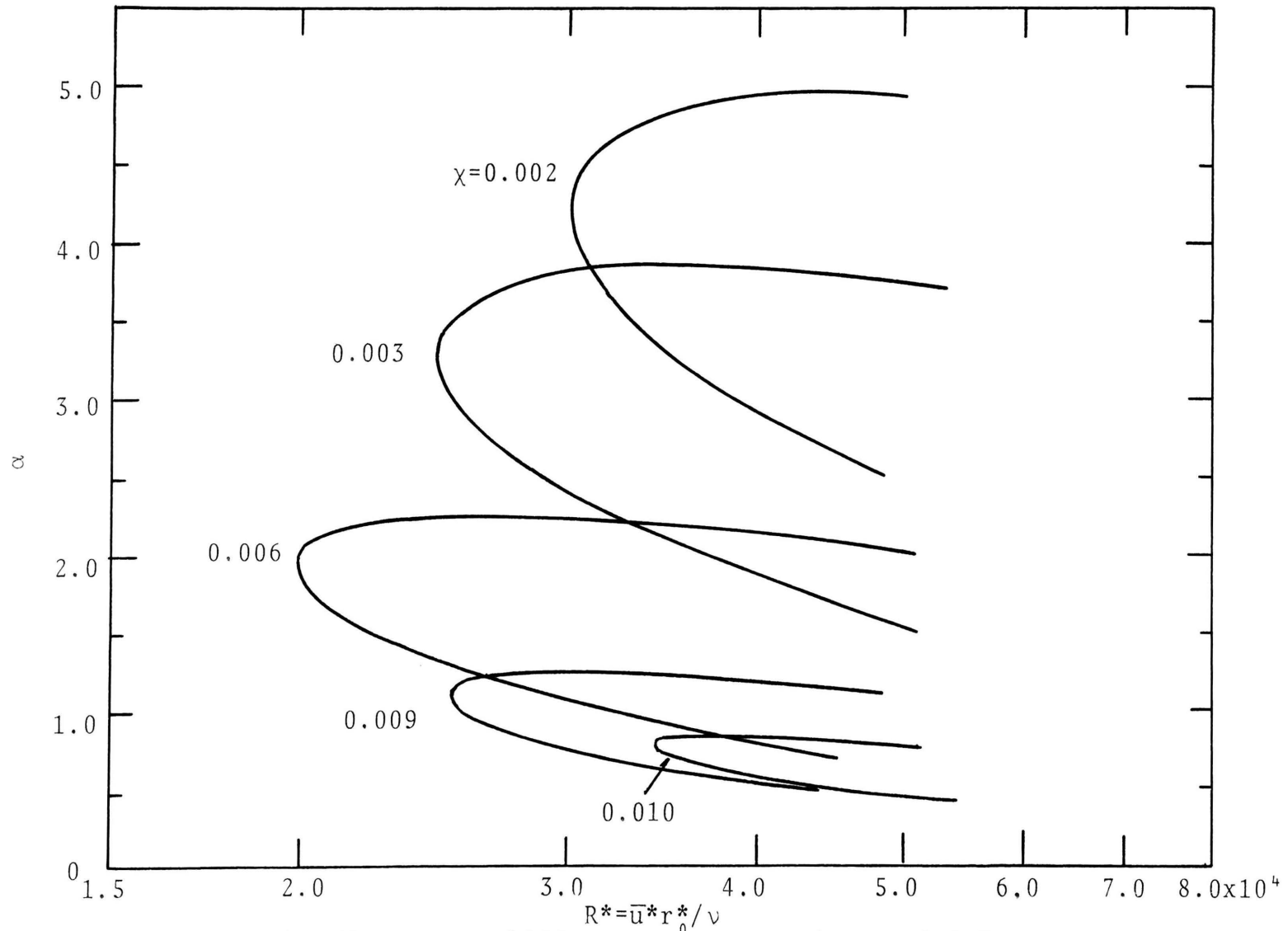


Figure 2. Neutral stability curves at various axial locations for axisymmetric disturbances $n=0$.

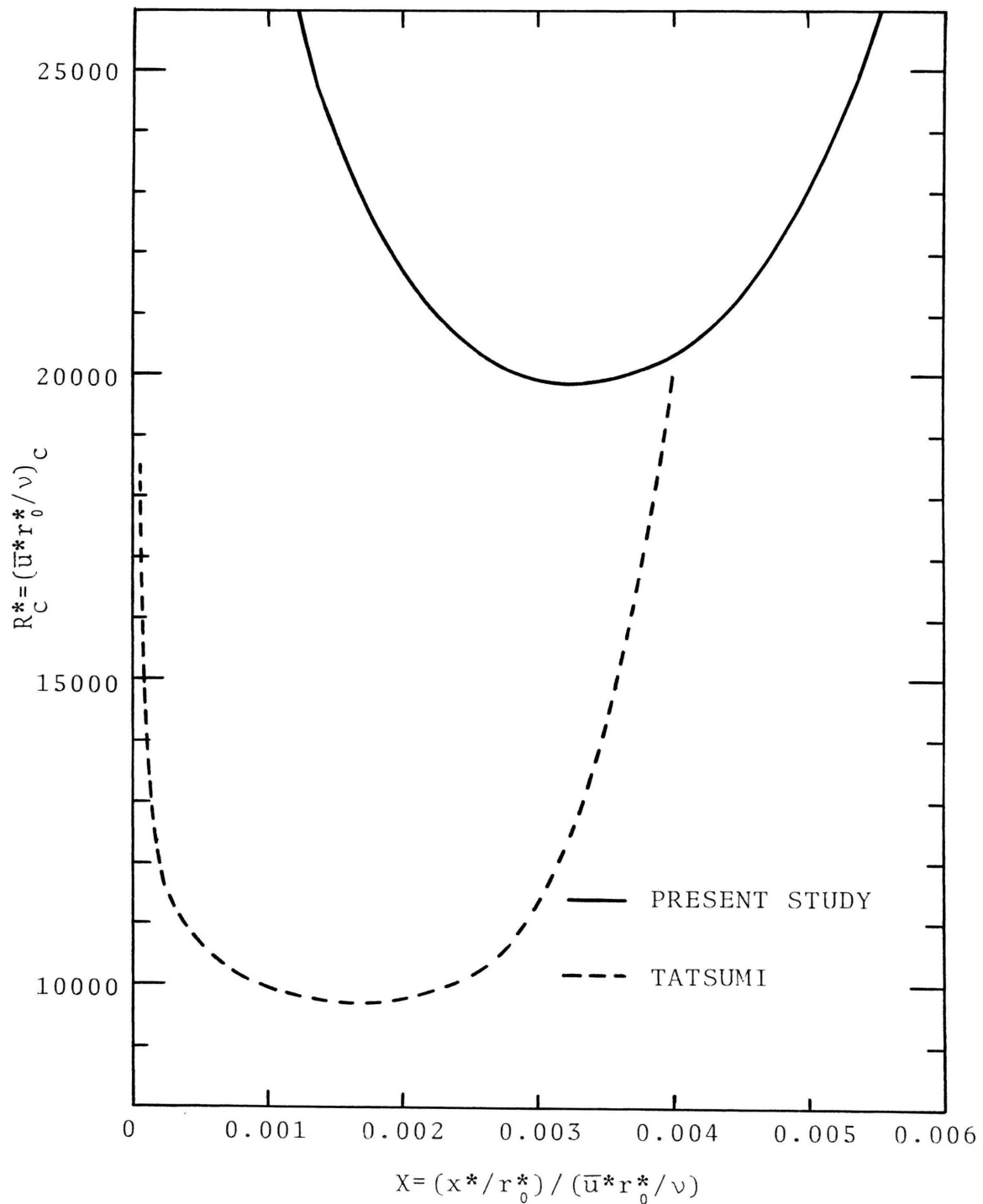


Figure 3. Axial variation of critical Reynolds number for axisymmetric disturbances $n=0$.

farther downstream, attaining infinity for the fully developed Poiseuille flow. This is to be contrasted with the case of developing flow in a parallel-plate channel in which the critical Reynolds number decreases monotonically as χ increases (41)

The stability results of Tatsumi are compared with those of the present investigation in Figure 3, which are shown in a dashed line. Tatsumi predicted a minimum critical Reynolds number of about 9700 at $X=0.00175$ which for this Reynolds number gives $x^*/r_0^*=17$. As can be seen, there is a big difference in the minimum critical Reynolds numbers between the two solutions. However, as pointed out earlier, Tatsumi's results are doubtful, for he used an inferior main flow velocity distribution and, as pointed out by Chen (23), there was an error in his main flow solution. For this reason, the present results are believed to be more accurate.

2. The Neutral Stability Curves for Non-Axisymmetric Disturbances

The neutral stability curves for the case of non-axisymmetric disturbances are shown in Figure 4 for axial locations $\chi=0.015, 0.010, 0.006, 0.003$ and 0.002 . The variation of the critical Reynolds number with the axial position is illustrated in Figure 5. The computer outputs of the data for Figure 4 are tabulated in Table C-1 through

C-8, Appendix C. The data for Figure 5 are presented in Table D-2, Appendix D. As in the case of axisymmetric disturbances, Figure 4 and 5 reveal that the critical Reynolds number R_c decreases as the axial position increases, attains a minimum value of about 19780 at the location $X=0.00490$ (i.e., $\chi=0.008346$), and then increases monotonically to infinity as the axial distance increases toward the fully developed region.

D. Comparison of Results between Axisymmetric and Non-Axisymmetric Disturbances

Lessen, et al. (16) and Burrige (17) found that for Poiseuille pipe flow, instability does not exist but that the non-axisymmetric disturbances with $n=1$ is the most unstable among all axisymmetric and non-axisymmetric disturbances. In the present study, it was found that the flow in the entrance region of a circular tube is unstable to small disturbances for both axisymmetric and non-axisymmetric cases. The results from these two cases will now be compared.

In Figure 6, the neutral stability curves for both $n=0$ and $n=1$ at four locations are brought together. The solid curves are for the non-axisymmetric case ($n=1$) and the dashed curves are for the axisymmetric case ($n=0$). It is seen from the figure that for small χ values, the solid lines lie to the right of the dashed lines, indicating that the axisymmetric disturbances are more unstable than

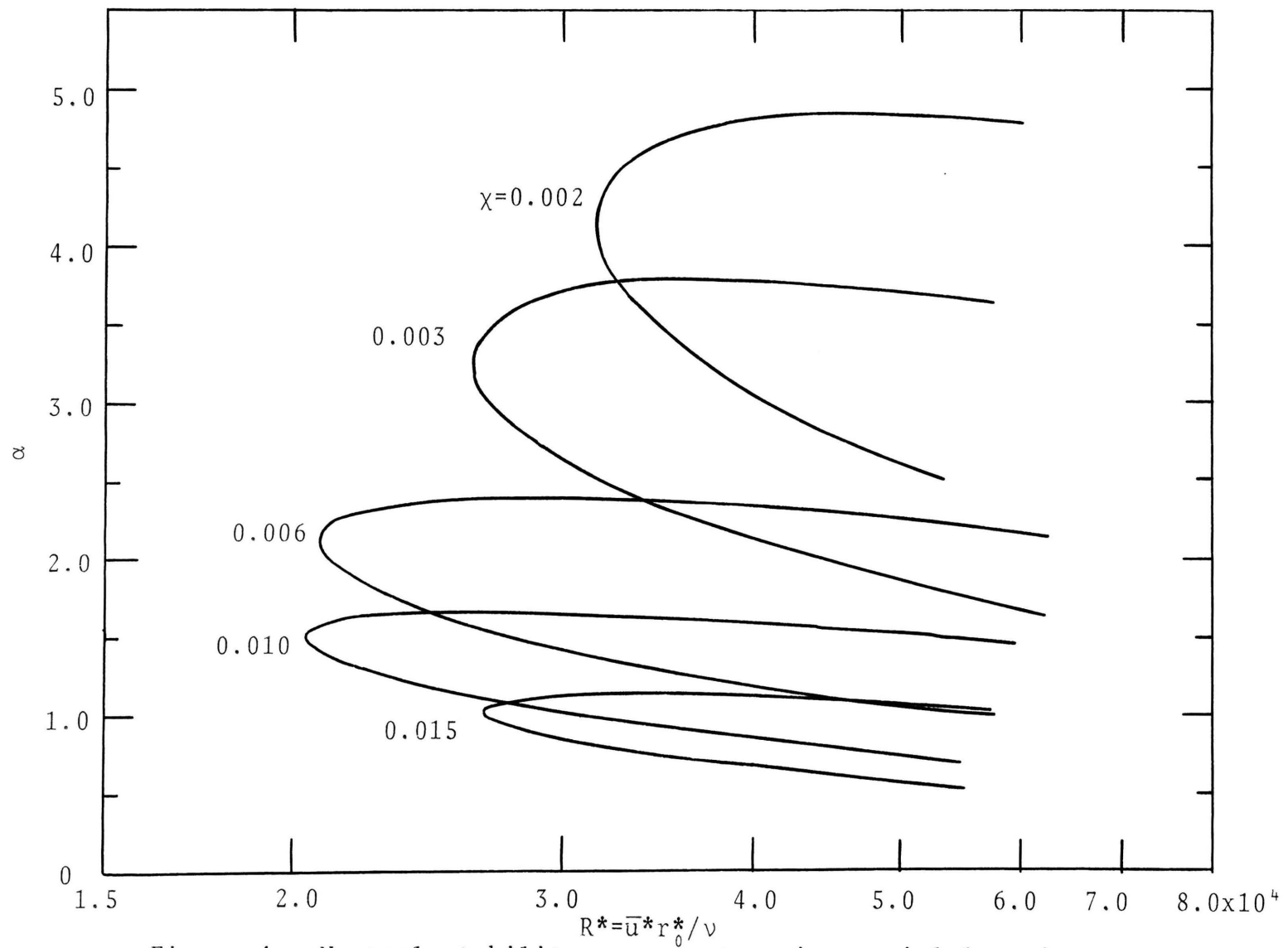


Figure 4. Neutral stability curves at various axial locations for non-axisymmetric disturbances $n=1$.

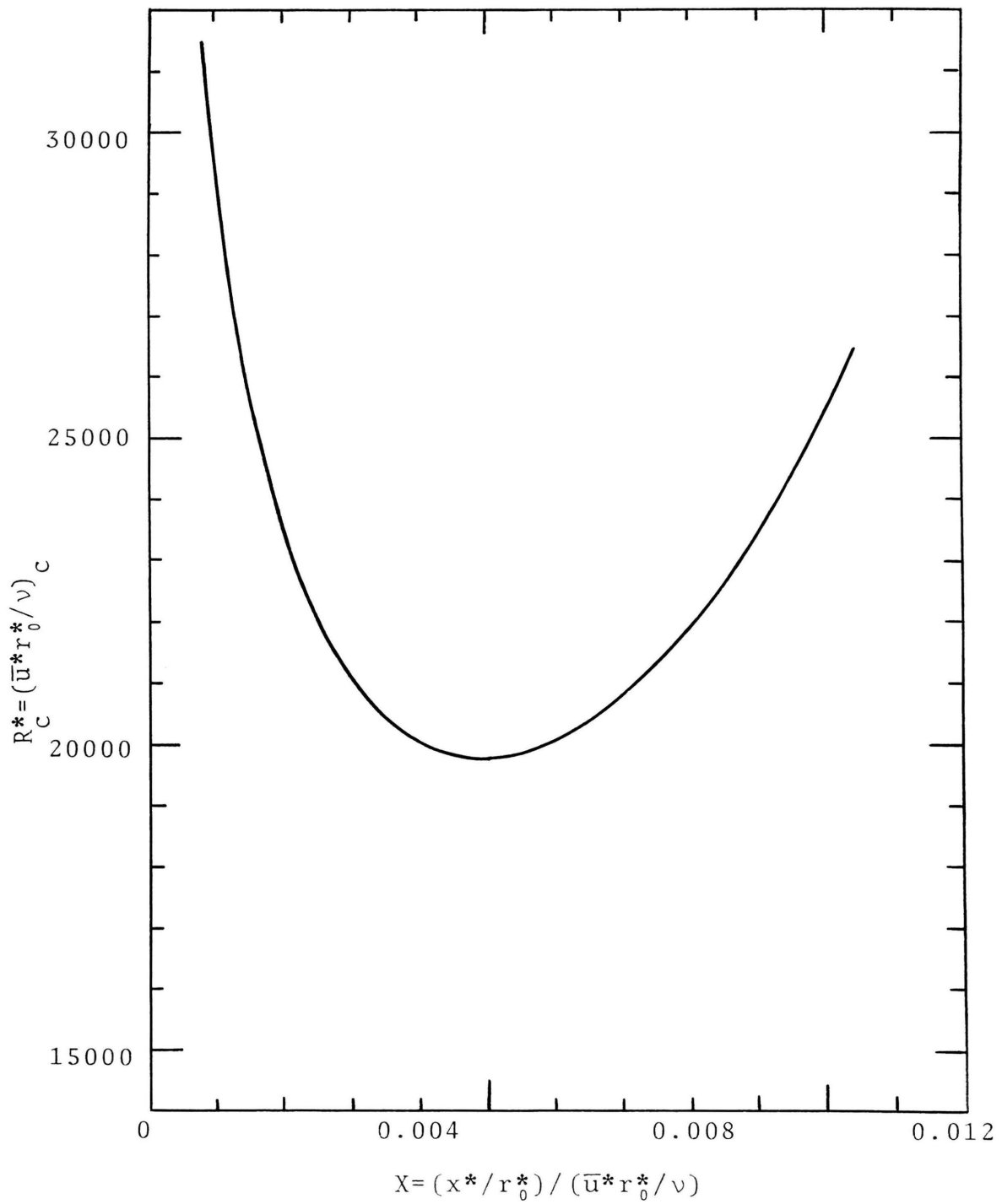


Figure 5. Axial variation of critical Reynolds number for non-axisymmetric disturbances $n=1$.

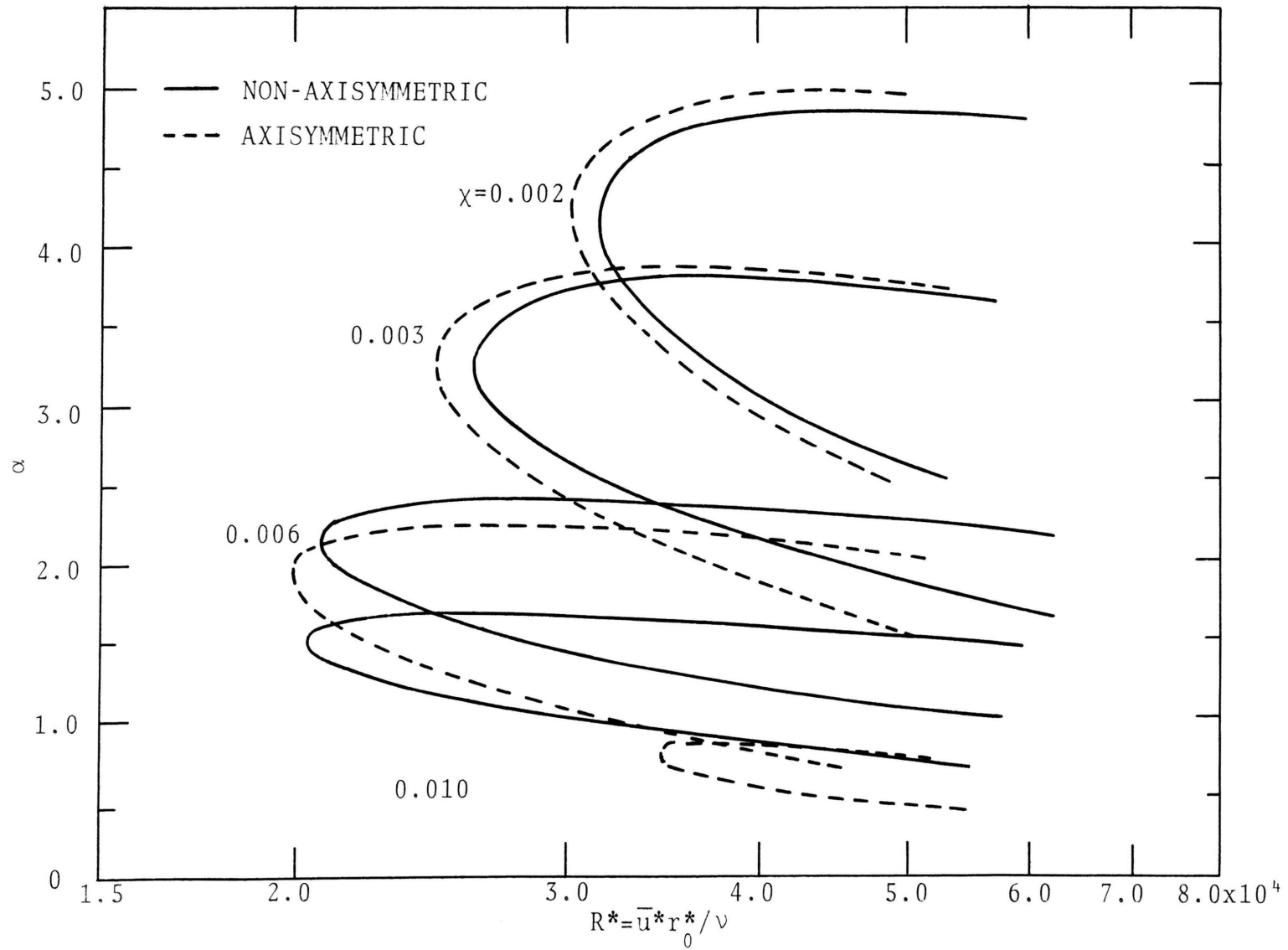


Figure 6. A comparison of neutral stability curves between axisymmetric and non-axisymmetric disturbances.

the non-axisymmetric disturbances. The opposite trend is in evidence for large χ values. This finding for large χ values agrees with the conclusion of Lessen, et al. and of Burrige for the Poiseuille pipe flow in the fully developed region.

The reason that axisymmetric disturbances are more unstable than the non-axisymmetric disturbances in the region with small χ values (that is, for the region close to the tube inlet) is probably due to the boundary layer effect in that region. In the region near the tube inlet, the boundary layer is developing along the tube wall and the flow is essentially of the boundary layer type. Thus, Squire's theorem (42) for plane parallel flow, which states that two dimensional disturbances are more unstable than three dimensional disturbances, applies.

The variation of critical Reynolds number R^* with physical axial coordinate X is compared in Figure 7 for $n=0$ and $n=1$. It is of interest to note that the two curves have a similar shape. The non-axisymmetric case has a somewhat lower minimum critical Reynolds number $R^*=19780$ (as compared to $R^*=19900$ for the axisymmetric case) which occurs at a large downstream distance $X=0.00490$ or $\chi=0.008346$ (as compared to $X=0.00325$ or $\chi=0.00629$). For X less than 0.0038, the axisymmetric disturbances are more unstable than the non-axisymmetric disturbances, while the opposite is true when X is larger than 0.0038.

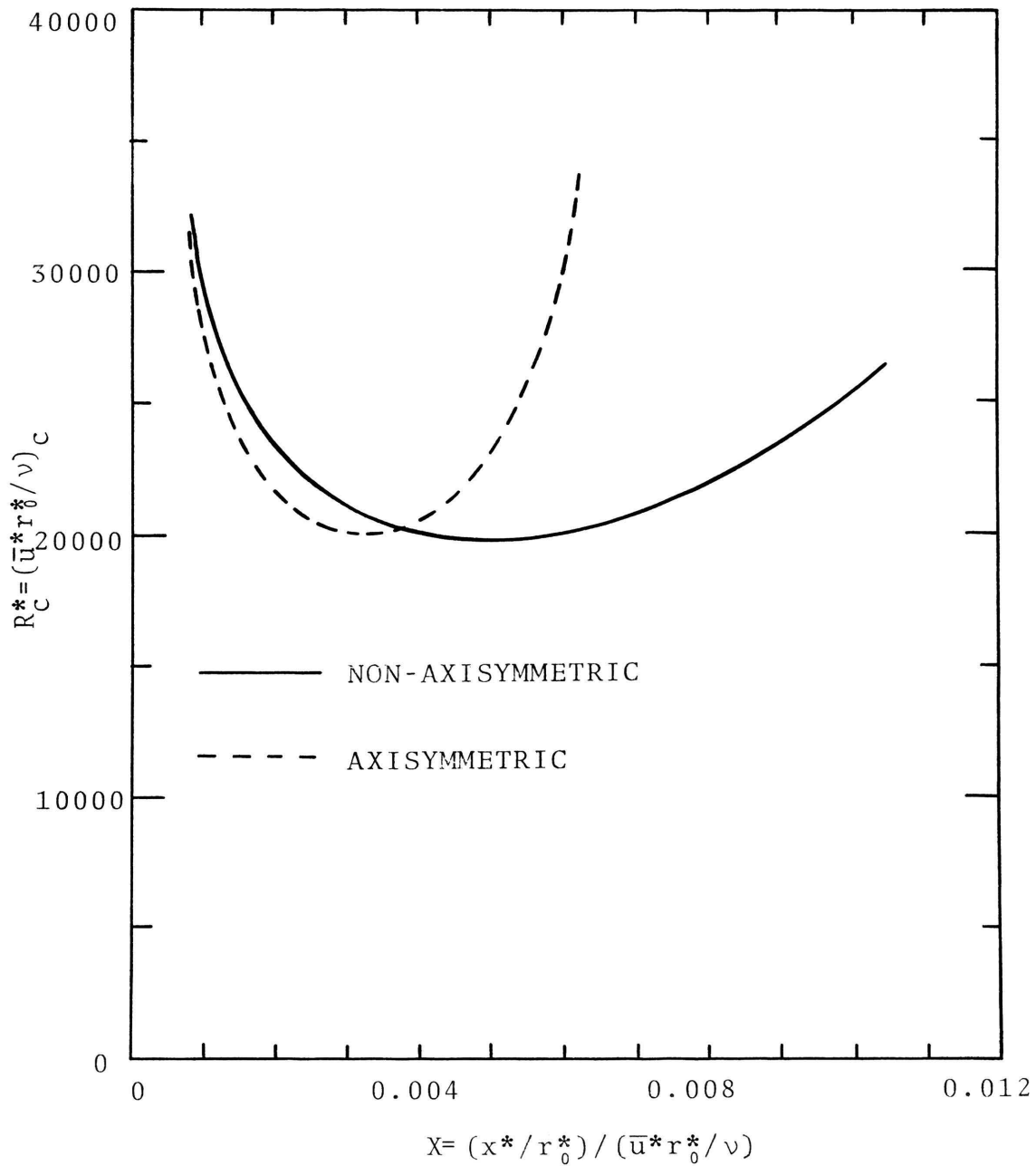


Figure 7. A comparison of axial variation of critical Reynolds number between axisymmetric and non-axisymmetric disturbances.

The axial variation of the critical wave number for $n=0$ and $n=1$ is shown in Figure 8. For both cases, α_c decreases monotonically as X increases. A decrease in the critical wave number implies an increase in the critical wave length of the disturbances, since $\alpha=2\pi/\lambda$.

E. Eigenfunction

In chapter III, the technique used in calculating the eigenfunctions was discussed. The numerical results for the eigenfunctions are presented in this section.

The eigenfunction ϕ and its first derivative ϕ' for the axisymmetric case $n=0$ at the axial location $X=0.006$ ($\chi=0.00323$) with $\alpha=1.9$, $R=23781$, $c_r=0.346436$ and $c_i=0$ are plotted in Figure 9. The eigenfunctions were computed by assigning the real part of the coefficient a_1 in equation (2-58) the normalizing value 1.0 and calculating the real and imaginary parts of a_2 and the imaginary part of a_1 , such that the boundary conditions (2-51) at tube wall are satisfied.

For the non-axisymmetric disturbances with $n=1$ in the fully developed region, the eigenfunctions u , v and w for $R=2200$, $\alpha=0.98$, $c_r=0.398348$ and $c_i=-0.0678317$ are plotted in Figure 10. These results are based on the solution which satisfies the three homogeneous boundary conditions (2-45) or (2-46) with a_1 , one of the three coefficient a_i ($i=1,2,3$), assigned the value of $(1.0+i0.0)$.

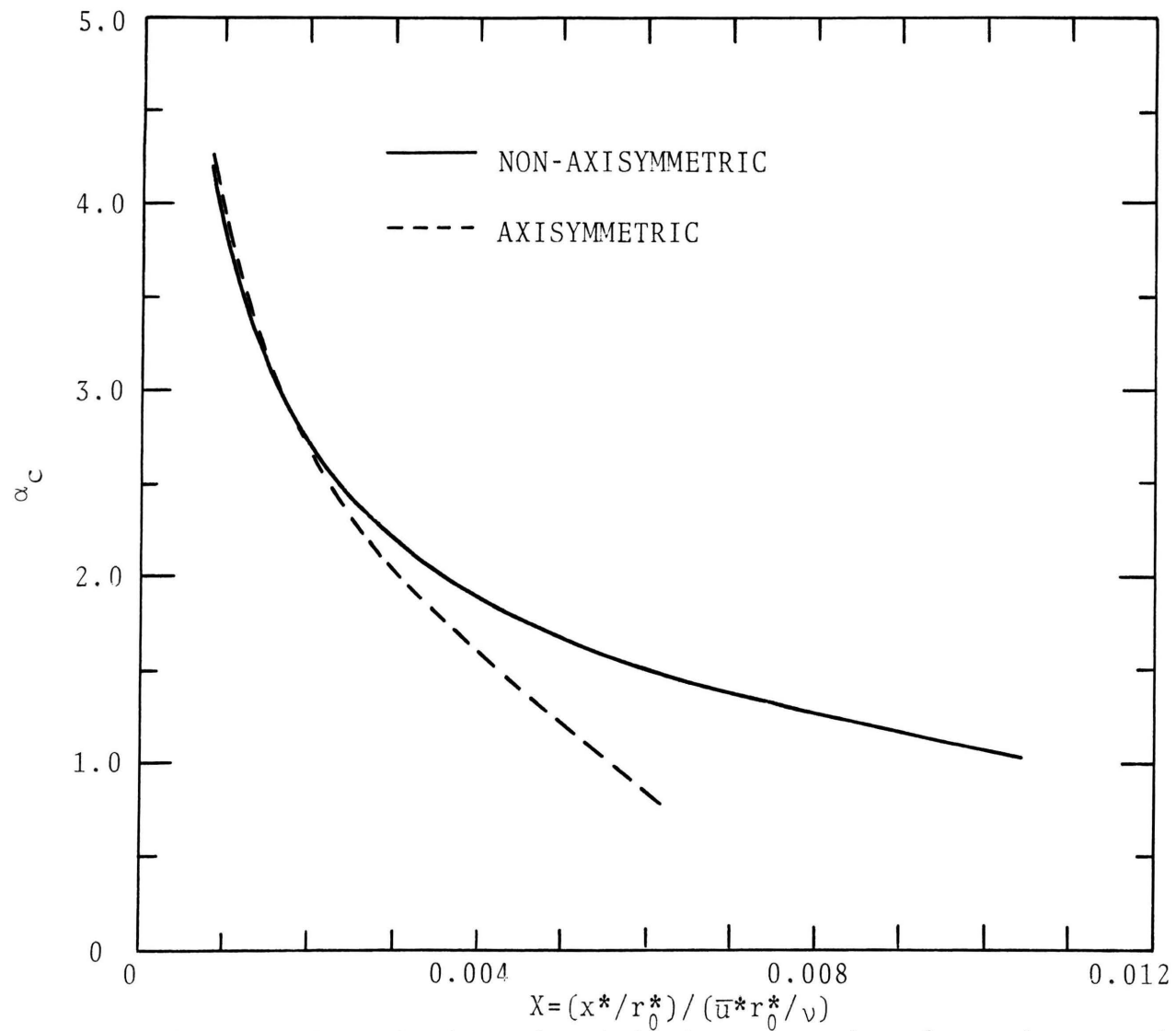


Figure 8. Axial variation of critical wave number for axisymmetric and non-axisymmetric disturbances.

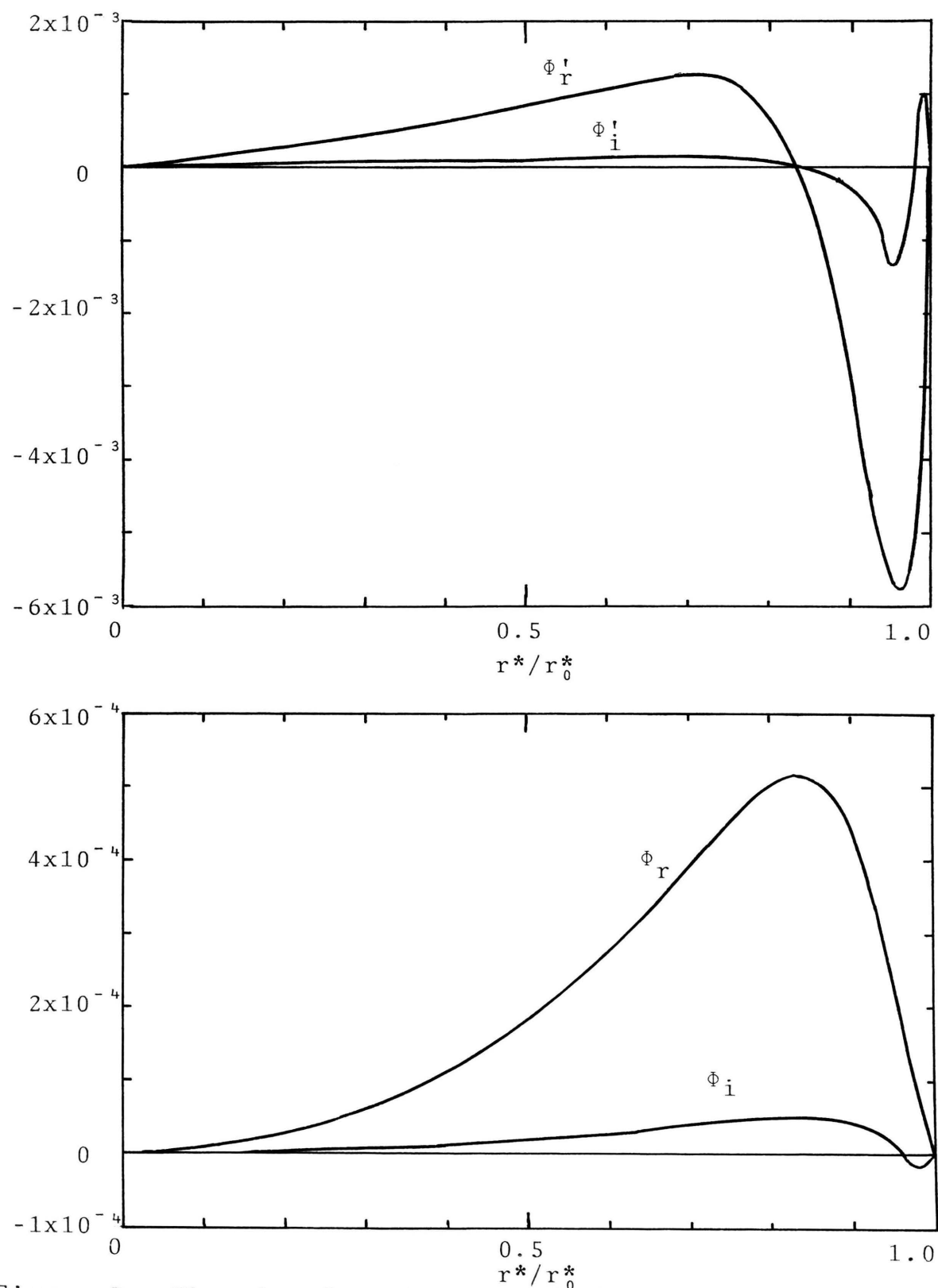


Figure 9. The eigenfunctions ϕ and ϕ' for $n=0$ at $\chi=0.006$; $\alpha=1.9$, $R=23781$, $c_r=0.346436$ and $c_i=0$.

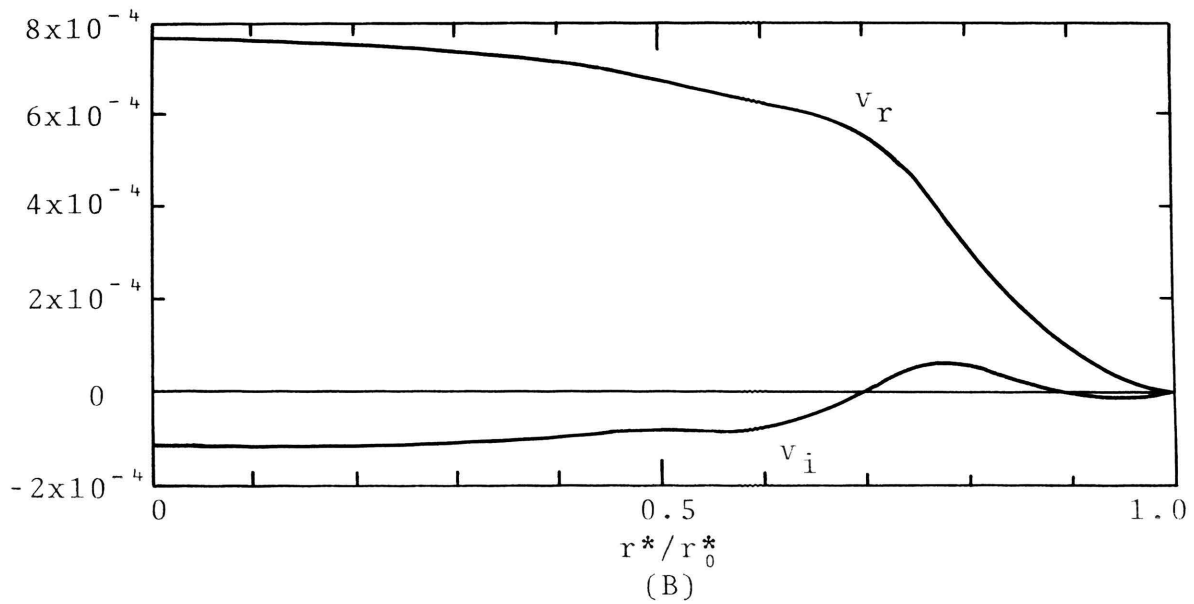
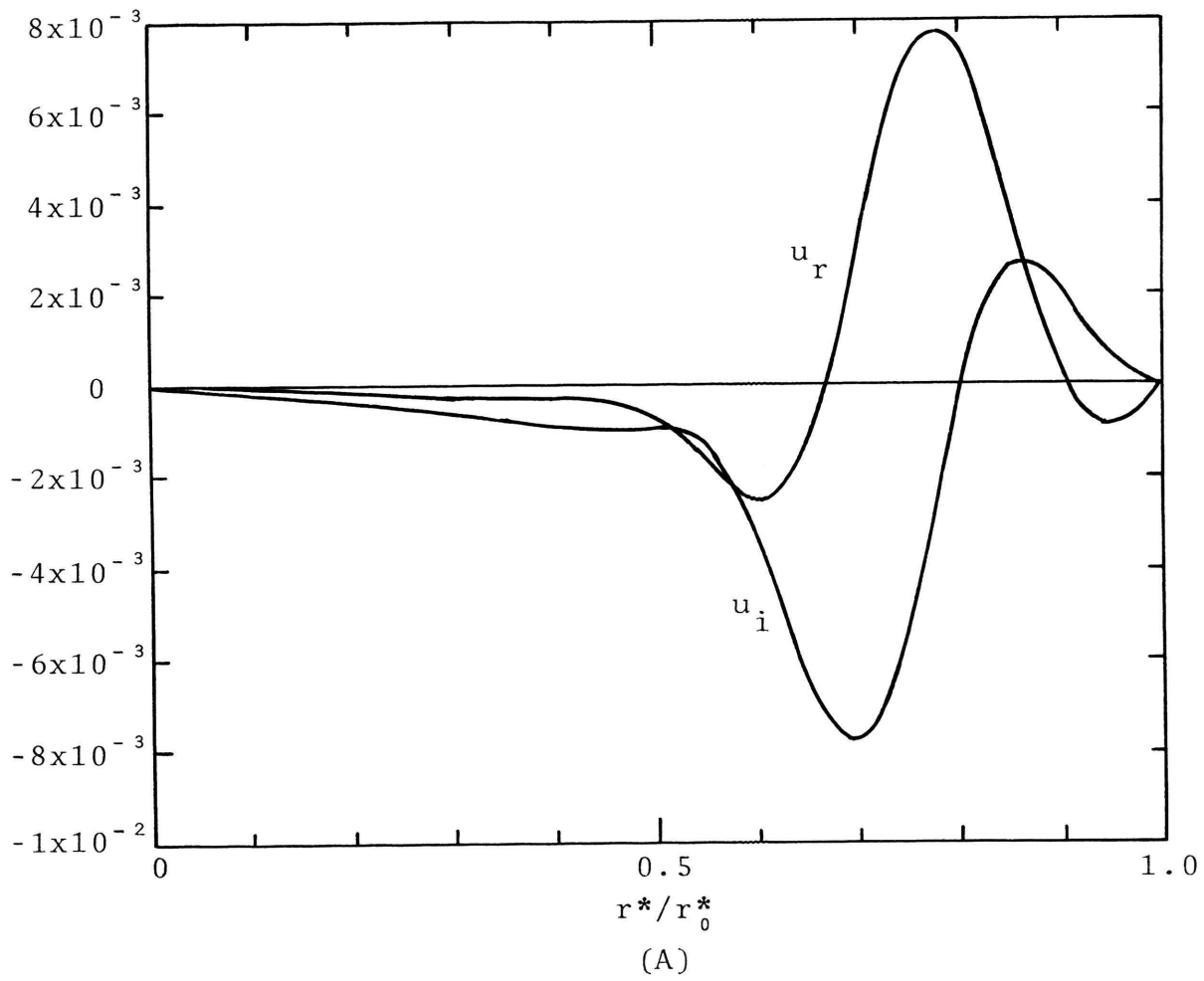


Figure 10 (A), (B). For legend see P.72

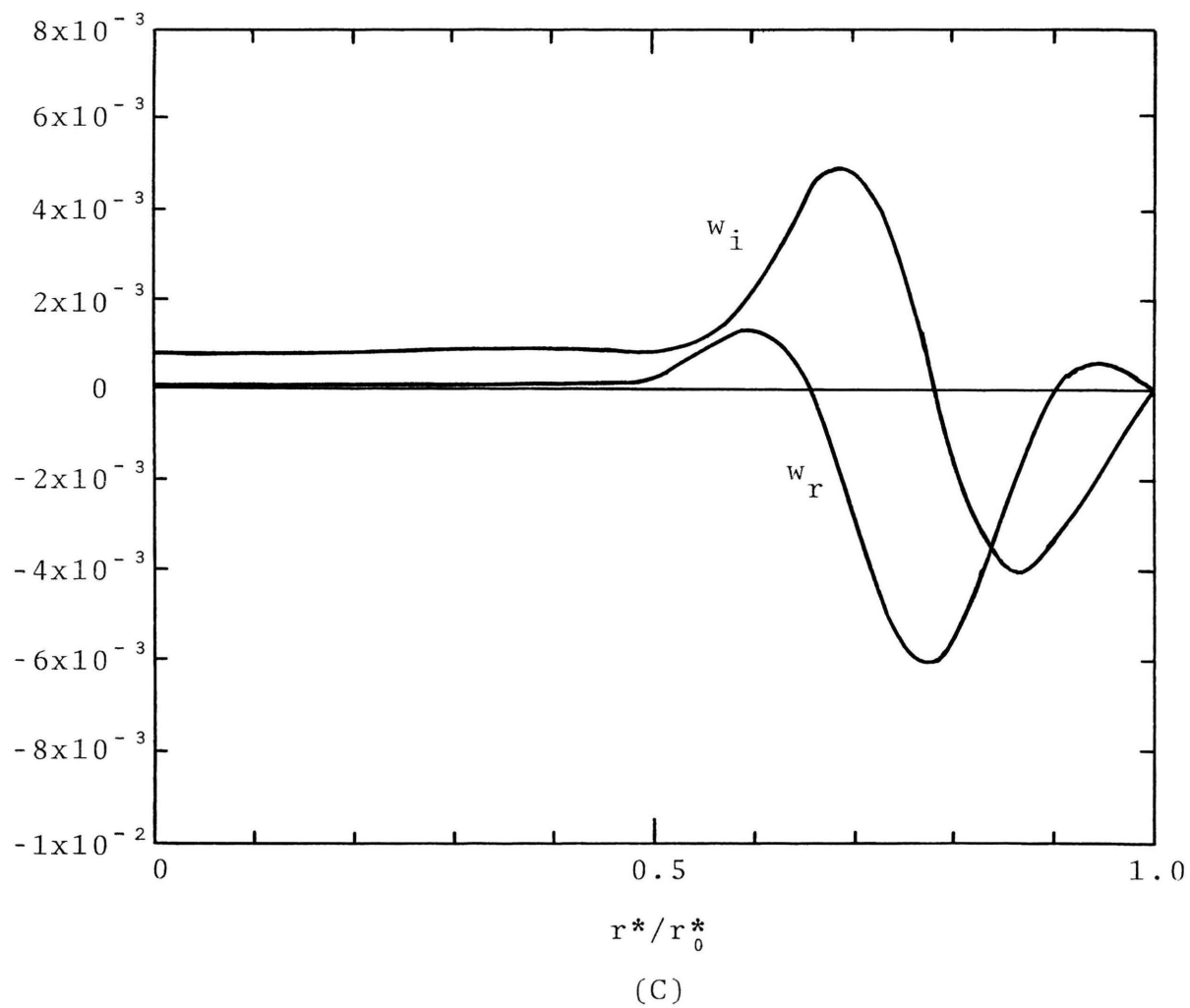
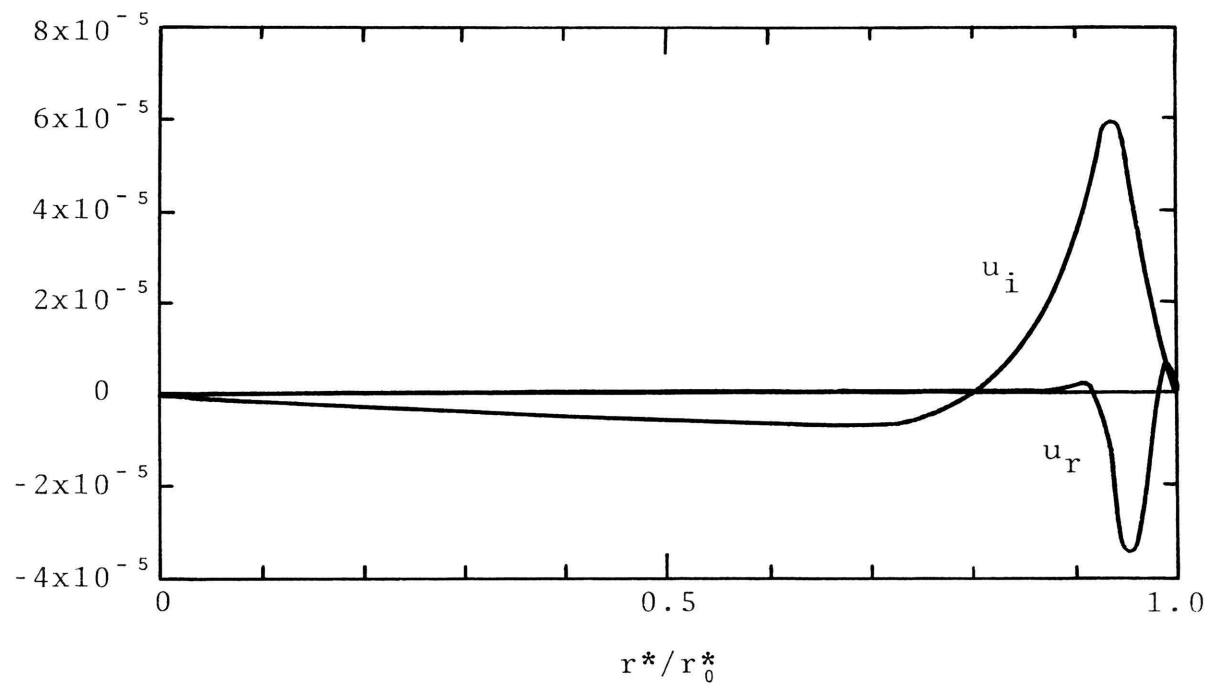
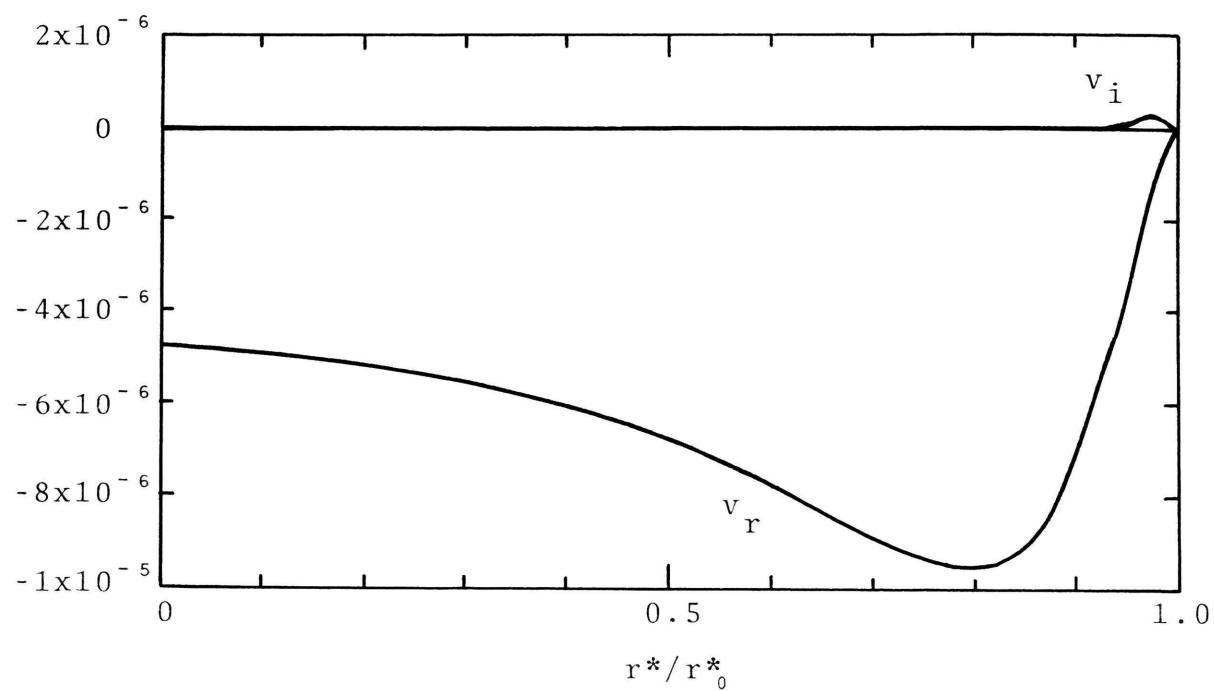


Figure 10. The eigenfunctions u , v and w for $n=1.0$ in fully developed region; $\alpha=0.98$, $R=2200$, $c_r=0.398348$ and $c_i=-0.0678317$.

The eigenfunctions u , v and w for the non-axisymmetric case $n=1$ with $R=25009$, $\alpha=2.0$, $c_r=0.325201$ and $c_i=0.0000166$ at a location $\chi=0.006$ ($x=0.00323$) in the entrance region are shown in Figure 11. The results are from the solution with $a_1=(1.0+i0.0)$ as the normalizing condition. The eigenfunction of this fixed wave number $\alpha=2.0$, but at different Reynolds numbers $R=23881$ ($c_r=0.327704$, $c_i=-0.000674$) and $R=26137$ ($c_r=0.322823$, $c_i=0.000634$) were also computed. They show only a slight change in magnitude as compared with those of $R=25009$ in Figure 11 and are, therefore, not presented.

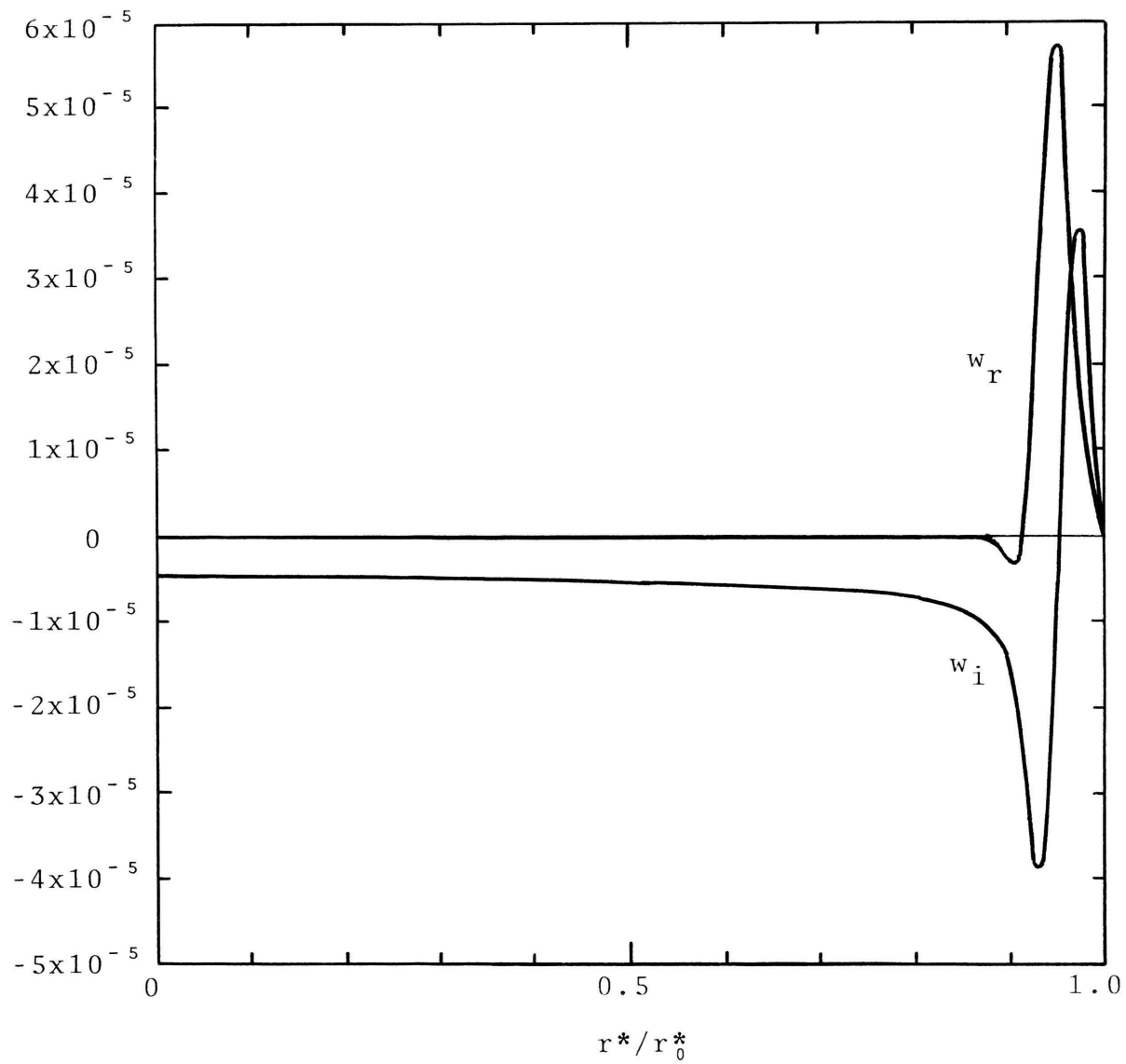


(A)



(B)

Figure 11 (A), (B). For legend see P.75



(C)

Figure 11. The eigenfunctions u , v and w for $n=1.0$ at $\chi=0.006$; $\alpha=2.0$, $R=25009$, $c_r=0.325201$ and $c_i=0.0000166$.

V. CONCLUSION

In this dissertation, the stability of laminar flow in the entrance region of a circular tube was investigated by using the linear perturbation theory of hydrodynamic stability. Both axisymmetric and non-axisymmetric disturbances were considered in the analysis. The main flow in the development region of the tube was treated as nearly parallel in the stability formulation. The governing equations for the disturbances and the corresponding boundary conditions constitute an eigenvalue problem. This eigenvalue problem was solved by a direct numerical integration of the disturbance equations along with an iteration technique. Two purification schemes, the filtering and the orthonormalization methods, were employed to remove the "parasitic errors" in solving the disturbance equations by using the fourth order Runge-Kutta integration scheme. The stability characteristics of the axisymmetric and non-axisymmetric disturbances were studied. The neutral stability curves, the axial variation of the critical Reynolds number, and the eigenfunctions were presented.

It is found that: (1) the flow in the entrance region of a circular tube is unstable to both axisymmetric and non-axisymmetric infinitesimal disturbances; (2) the critical Reynolds number for both cases decreases with an increase in the axial distance from the entrance,

attains a minimum value, and then increases monotonically to infinity as the axial distance increases farther to the fully developed flow region; (3) the minimum critical Reynolds number of 19900 (based on the tube radius and the average velocity) for the axisymmetric disturbances occurs at the axial location $X=0.00325$; (4) for the case of non-axisymmetric disturbances, the minimum critical Reynolds number of 19780 occurs at the axial location $X=0.0049$; (5) the non-axisymmetric disturbance is more stable than the axisymmetric disturbance in the region near the tube inlet; and (6) the axisymmetric disturbance is more stable than the non-axisymmetric disturbance in the region away from the entrance of the tube.

REFERENCE

1. Reynolds, O., "An Experimental Investigation of the Circumstances Which Determine Whether the Motion of Water Shall Be Direct Or Sinuous and the Law of Resistance in Parallel Channels," Phil. Trans. Roy. Soc., 174, 935 (1883)
2. Rayleigh, Lord, "On the Stability Or Instability of Certain Fluid Motions, I," Scientific Papers, 1, 474 (1880)
3. Rayleigh, Lord, "On the Stability Or Instability of Certain Fluid Motions, II," Scientific Papers, 3, 2 (1887)
4. Ekman, V.W., (1910), see Schlichting (9)
5. Kuethe, A.M., "Some Features of Boundary Layers and Transition to Turbulent Flow", Journal of Aeronautical Science, 23, 444 (1956)
6. Leite, R.J., "An Experimental Investigation of the Stability of Poiseuille Flow," Journal of Fluid Mechanics, 5, 81 (1959)
7. Bhat, W.V., "An Experimental Investigation of the Stability of Hagen-Poiseuille Flow Subjected to the First Mode of Azimuthally Periodic Small Disturbance," Ph.D. Thesis, University of Rochester, (1966)
8. Houlihan, T.M., "A Theoretical and Experimental Investigation of the Stability of Pipe Flow with Respect to three Dimensional Disturbances," Ph.D. Thesis, Department of Mechanical Engineering, Syracuse University, (1969)
9. Schlichting, H., Boundary Layer Theory, Chapters 16,17 and 20, McGraw-Hill, New York (1968)
10. Sexl, T., "Über Dreidimensionale Störungen der Poiseuilleschen Strömung," Annalen Der Physik, 84, 807 (1927)
11. Pretsch, T., "Über die Stabilität einer Laminarströmung in einem Geraden Rohr mit Kreisförmigen Querschnitt," Z. Angew, Math. Mech., 21, 204 (1941)

12. Pekeris, C.L., "Stability of the Laminar Flow through a Straight Pipe of Circular Cross-Section to Infinitesimal Disturbances Which Are Symmetric about the Axis of the Pipe," Proc. Nat. Acad. of Sci., Wash. D.C., 34, 285 (1948)
13. Corcos, G.M. and Sellars, J.R., "On the Stability of Fully Developed Flow in a Pipe," J. Fluid Mech., 5, 97 (1959)
14. Schensted, see Gill (19), Univ. Mich. Engng. Coll. Tech. Rep. (1960)
15. Davey, A. and Drazin, P.G., "The Stability of Poiseuille Flow in a Pipe," J. Fluid Mech., 36, 209 (1969)
16. Lessen, M. and Sadler, S.G. and Liu, T.Y., "Stability of Pipe Poiseuille Flow," Phys. Fluids, 11, 1404 (1968)
17. Burrige, D.M., "The Stability Poiseuille Pipe Flow to Non-Axisymmetric Disturbances," Technical Report No.34, Florida State University (1970)
18. Salwen, H. and Grosch, C.E., "The Stability of Poiseuille Flow in a Pipe of Circular Cross-Section," J. Fluid Mech., 54, 93 (1972)
19. Gill, A.E., "On the Behavior of Small Disturbances to Poiseuille Flow in a Circular Pipe," J. Fluid Mech., 21, 145 (1965)
20. Garg, V.K. and Rouleau, W.T., "Linear Spatial Stability of Pipe Poiseuille Flow," J. Fluid Mech., 54, 113 (1972)
21. Graebel, W.P., "The Stability of Pipe Flow, Part 1, Asymptotic Analysis for Small Wave Numbers," J. Fluid Mech., 43, 270 (1970)
22. Tatsumi, T., "Stability of the Laminar Inlet Flow Prior to the Formulation of Poiseuille Regime," J. Phys. Soc. Japan, 7, 489 (1952)
23. Chen, B.H.P., "Finite Amplitude Disturbances in the Stability of Pipe Poiseuille Flow," Ph.D. Thesis, The University of Rochester (1969)
24. Kaplan, R.E., "The Stability of Laminar Incompressible Boundary Layer in the Presence of Compliant Boundaries," ASRL, TR 116-1, MIT, (1964)

25. Wazzan, A.R., Okamura, T.T. and Smith, A.M.O., "Stability of Laminar Boundary Layer at Separation," Phys. Fluids, 10, 2540 (1967)
26. Sparrow, E.M., Lin, S.H. and Lundgren, T.S., "Flow Development in the Hydrodynamic Entrance Region of Tubes and Ducts," Phys. Fluids, 7, 338 (1964)
27. IBM System/360 Scientific Subroutine Package, (360A-CM-03X) Version II (1967)
28. Abramowitz, M. and Stegun, L., "Handbook of Mathematical Functions," pp. 369-370, 5th Edition, Dover Publications Inc., New York (1968)
29. Batchelor, G.K. and Gill, A.E., "Analysis of the Stability of Axisymmetric Jets," J. Fluid Mech., 14, 529 (1962)
30. Gersting, J.M., Jr., "The Hydrodynamic Stability of Two Axisymmetric Annular Flows," Ph.D. Thesis, Arizona State University (1970)
31. Kurtz, E.F. and Crandall, S.H., "Computer-Aided Analysis of Hydrodynamic Stability," Journal of Mathematics and Physics, XLI, No. 4, 264 (1962)
32. Thomas, L.M., "The Stability of Plane Poiseuille Flow," Physical Review, 91, 780 (1953)
33. Chen, T.S., "Hydrodynamics Stability of Developing Flow in a Parallel-Plate Channel," Ph.D. Thesis, Dept. of Mechanical Engineering, University of Minnesota (1966)
34. Lee, L.H. and Reynolds, W.C., "On the Approximate and Numerical Solution of Orr-Sommerfield Problems," Quart. J. Mech. and Appl. Math., XX, Part 1, (1967)
35. Nachtsheim, P.R., "An Initial Value Method for the Numerical Treatment of the Orr-Sommerfield Equation for the Case of Plane Poiseuille Flow," NASA TN D-2414 (1964)
36. Conte, S.D., "The Numerical Solution of Linear Boundary Value Problem," SIAM Review 8, 309 (1966)
37. Davey, A. and Nguyen, H.P.G., "Finite-Amplitude Stability of Pipe Flow," J. Fluid Mech., 45, 701

38. Collatz, L., "The Numerical Treatment of Differential Equations", Third Edition, Spring-Verlag, New York (1966)
39. Muller, D.E., "A Method for Solving Algebraic Equations Using an Automatic Computer", Mathematical Tables and Other Aids to Computations, 10, 208 (1956)
40. Liu, T.Y., "An Analytical Investigation of the Stability of Hagan-Poiseuille Flow Subjected to Three-Dimensional Infinitesimal Disturbances", Ph.D. Thesis, The University of Rochester (1968)
41. Chen, T.S. and Sparrow, E.M., "Stability of the Developing Laminar Flow in a Parallel-Plate Channel", J. Fluid Mech., 30, 209 (1967)
42. Squire, H.B., "On the Stability for Three-Dimensional Disturbances of Viscous Fluid Flow Between Parallel Walls", Proc. Roy. Soc., London, A142, 621 (1933)

VITA

The author, Lung-mau Huang, was born on September 7, 1940, in Kaohsiung, Taiwan.

He was graduated from Kaohsiung High School, Taiwan in 1959. He entered National Taiwan University in September 1960 and received his Bachelor of Science degree in Mechanical Engineering in June, 1964. After his graduation from the university, he served one year under the ROTC program in the Nationalist Chinese Navy. From September 1965 to February 1967, he taught both at Fu-hsin and Kaohsiung Technical Schools in Taiwan.

In June 1967, he enrolled in the Graduate School of the University of Missouri-Rolla. He received his Master of Science degree in August 1968. Since then he has been pursuing the Doctor of Philosophy degree in Mechanical Engineering.

APPENDICES

Appendix A

Table A-1

The Relationship among χ , ϵ and X

χ	X	ϵ	χ	X	ϵ
0.0	0.0	0.36400	0.027	0.02286	1.14559
0.001	0.00040	0.43488	0.028	0.02401	1.16211
0.002	0.00087	0.50014	0.029	0.02518	1.17827
0.003	0.00140	0.55121	0.030	0.02637	1.19409
0.004	0.00197	0.59490	0.031	0.02757	1.20958
0.005	0.00258	0.63385	0.032	0.02879	1.22474
0.006	0.00323	0.66743	0.033	0.03002	1.23958
0.007	0.00392	0.70242	0.034	0.03127	1.25412
0.008	0.00464	0.73337	0.035	0.03253	1.26835
0.009	0.00539	0.76262	0.036	0.03380	1.28228
0.010	0.00616	0.79045	0.037	0.03509	1.29591
0.011	0.00697	0.81705	0.038	0.03640	1.30926
0.012	0.00780	0.84258	0.039	0.03771	1.32232
0.013	0.00865	0.86715	0.040	0.03904	1.33511
0.014	0.00953	0.89087	0.045	0.04586	1.39499
0.015	0.01043	0.91381	0.050	0.05297	1.44844
0.016	0.01136	0.93605	0.060	0.06792	1.53789
0.017	0.01231	0.95763	0.070	0.08366	1.60711
0.018	0.01327	0.97862	0.080	0.10000	1.65985
0.019	0.01426	0.99904	0.090	0.11681	1.69964
0.020	0.01527	1.01893	0.100	0.13396	1.72950
0.021	0.01630	1.03833	0.150	0.22254	1.79763
0.022	0.01735	1.05726	0.200	0.31292	1.81420
0.023	0.01841	1.07575	0.250	0.40376	1.81843
0.024	0.01950	1.09380	0.300	0.49472	1.81954
0.025	0.02060	1.11145	0.350	0.58570	1.81983
0.026	0.02172	1.12871	0.400	0.67670	1.81991

Appendix B
 Tables of Neutral Stability Results for
 Axisymmetric Disturbances

Table B-1
 Neutral Stability Results for $n=0$ at
 $\chi=0.002$, $U_{\max}=1.10722$, $N=200$

α	R	R*	(c_r)	$(c_r)^*$
2.50	53847	48634	0.296002	0.327730
2.75	47590	42982	0.303343	0.335858
3.00	42827	38683	0.310138	0.343382
3.50	36573	33032	0.321617	0.356091
4.00	33631	30375	0.329402	0.364711
4.19	33338	30110	0.331058	0.366582
4.25	33361	30131	0.331381	0.366901
4.50	34209	30897	0.331414	0.366938
4.75	36400	32876	0.329006	0.364272
4.80	38726	34976	0.326058	0.361007
4.9018	45000	40643	0.318291	0.352408
4.8968	55000	49675	0.307566	0.340533

Table B-2
 Neutral Stability Results for $n=0$ at
 $\chi=0.003$, $U_{\max}=1.13312$, $N=200$

α	R	R*	(c_r)	$(c_r)^*$
1.5	58600	51717	0.296537	0.336004
2.0	41646	36754	0.310822	0.352190
2.5	32819	28964	0.323807	0.366903
2.75	30235	26683	0.329133	0.372937
3.00	28608	25248	0.333281	0.377638
3.25	27939	24658	0.335811	0.380504
3.28	27897	24620	0.336043	0.380775
3.50	28534	25182	0.335851	0.380550
3.75	32145	28424	0.330322	0.374284
3.8456	40000	35302	0.318714	0.361132
3.8070	50000	44127	0.306757	0.347584
3.7259	60000	52953	0.297178	0.336730

Table B-3
 Neutral Stability Results for $n=0$ at
 $\chi=0.005$, $U_{\max}=1.17564$, $N=150$

α	R	R*	(c_r)	$(c_r)^*$
1.75	27273	23198	0.338657	0.398133
2.00	24940	21214	0.342028	0.402096
2.25	23965	20384	0.343505	0.403833
2.26	23960	20380	0.343469	0.403796
2.50	25199	21434	0.340308	0.400074

Table B-4
 Neutral Stability Results for $n=0$ at
 $\chi=0.006$, $U_{\max}=1.19420$, $N=150$

α	R	R*	(c_r)	$(c_r)^*$
0.7	53775	45030	0.333746	0.398556
1.0	37939	31770	0.337811	0.403410
1.3	29860	25004	0.342117	0.408552
1.6	25511	21362	0.345586	0.412695
1.7	24649	20640	0.346291	0.413537
1.8	24063	20150	0.346622	0.413933
1.9	23781	19914	0.346434	0.413707
1.93	23765	19900	0.346250	0.413491
2.0	23881	19998	0.345479	0.412567
2.1317	25000	20935	0.342101	0.408533
2.2272	28000	23447	0.335218	0.400314
2.2461	35000	29309	0.322760	0.385436
2.1750	45000	37682	0.309674	0.369810
2.0838	55000	46056	0.299864	0.358094

Table B-5
 Neutral Stability Results for $n=0$ at
 $\chi=0.007$, $U_{\max}=1.21157$, $N=150$

α	R	R*	(c_r)	$(c_r)^*$
1.0	33186	27391	0.347188	0.420640
1.25	27744	22899	0.349123	0.422984
1.50	24995	20631	0.349566	0.423521
1.55	24732	20414	0.349307	0.423207
1.60	24577	20286	0.348867	0.422674
1.635	24534	20250	0.348450	0.422166
1.65	24547	20261	0.348195	0.421860
1.70	24672	20363	0.347218	0.420675
1.75	25004	20638	0.345810	0.418970

Table B-6
 Neutral Stability Results for $n=0$ at
 $\chi=0.009$, $U_{\max}=1.24367$, $N=150$

α	R	R*	(c_r)	$(c_r)^*$
0.40	67090	53946	0.355402	0.442003
0.50	54381	43727	0.355417	0.442018
0.60	46107	37074	0.355345	0.441928
0.70	40414	32496	0.355119	0.441647
0.80	36599	29267	0.354644	0.441056
0.90	33598	27015	0.353769	0.439969
1.00	31812	25580	0.352237	0.438063
1.095	31110	25015	0.349683	0.434888
1.100	31118	25021	0.349481	0.434636
1.200	32594	26208	0.343328	0.426983
1.2284	35000	28143	0.338355	0.420799
1.2260	40000	32163	0.330893	0.411518
1.1642	50000	40204	0.320541	0.398645
1.0891	60000	48245	0.313306	0.389646

Table B-7
 Neutral Stability Results for $n=0$ at
 $\chi=0.010$, $U_{\max}=1.25870$, $N=100$

α	R	R*	(c_r)	$(c_r)^*$
0.4	68228	54206	0.355578	0.447563
0.5	56112	44580	0.354680	0.446431
0.6	48620	38627	0.353253	0.444637
0.7	44137	35066	0.350878	0.441646
0.725	43435	34508	0.350027	0.440575
0.750	42923	34102	0.349010	0.439295
0.775	42641	33878	0.347758	0.437720
0.785	42594	33840	0.347191	0.437008
0.800	42681	33909	0.346139	0.435681
0.85	43302	34402	0.343801	0.432739
0.8439	45000	35751	0.340489	0.428570
0.8485	47000	37340	0.337735	0.425103
0.8231	55000	43696	0.330259	0.415694
0.7687	65000	51641	0.324181	0.408043

Appendix C
 Tables of Neutral Stability Results for
 Non-Axisymmetric Disturbances

Table C-1
 Neutral Stability Results for $n=1.0$ at
 $\chi=0.002$, $U_{\max}=1.10722$, $N=200$

α	R	R*	(c_r)	$(c_r)^*$
2.50	58815	53119	0.286061	0.316733
2.75	50862	45937	0.296151	0.327904
3.00	45125	40755	0.304880	0.337569
3.50	38113	34422	0.318439	0.352582
3.70	36441	32912	0.322500	0.357078
3.80	35840	32370	0.324196	0.358956
3.90	35379	31953	0.325667	0.360585
4.00	35061	31665	0.326900	0.361950
4.10	34911	31531	0.327851	0.363003
4.135	34888	31510	0.328136	0.363319
4.20	34934	31551	0.328505	0.363727
4.40	35531	32091	0.328825	0.364082
4.60	37573	33934	0.326887	0.361936
4.7932	44000	39839	0.319204	0.353428
4.8209	55000	49674	0.307401	0.340359
4.7555	66000	59609	0.297696	0.329614

Table C-2
 Neutral Stability Results for $n=1.0$ at
 $\chi=0.003$, $U_{\max}=1.13312$, $N=200$

α	R	R*	(c_r)	$(c_r)^*$
1.50	82533	72937	0.256284	0.290338
2.00	49151	43377	0.312132	0.353683
2.90	31142	27484	0.324232	0.367734
3.10	29986	26463	0.328206	0.371897
3.24	29710	26220	0.330029	0.373960
3.30	29794	26294	0.330326	0.374299
3.50	30720	27111	0.330152	0.374102
3.70	34443	30396	0.325108	0.368386
3.7715	40000	35301	0.317398	0.359650
3.7577	50000	44126	0.305516	0.346186
3.6522	65000	57364	0.291685	0.330513

Table C-3
 Neutral Stability Results for $n=1.0$ at
 $\chi=0.005$, $U_{\max}=1.17564$, $N=150$

α	R	R*	(c_r)	$(c_r)^*$
2.000	28061	23869	0.318858	0.374862
2.100	26910	22890	0.322694	0.379371
2.200	26120	22218	0.325802	0.383026
2.300	25684	21847	0.328097	0.385725
2.363	25605	21780	0.329058	0.386854
2.400	25639	21808	0.329442	0.387305
2.500	26104	22204	0.329560	0.387444
2.600	27606	23482	0.327478	0.384996

Table C-4

Neutral Stability Results for $n=1.0$ at $\chi=0.006$, $U_{\max}=1.19420$, $N=150$

α	R	R*	(c_r)	$(c_r)^*$
1.00	67713	56702	0.256976	0.306880
1.25	45270	37909	0.280297	0.334730
1.50	33743	28256	0.300085	0.358362
1.65	29643	24822	0.309828	0.369997
1.90	25730	21545	0.322007	0.384541
2.00	25009	20942	0.325211	0.388367
2.103	24720	20700	0.327397	0.390977
2.15	24800	20767	0.327877	0.391551
2.25	25610	21445	0.327397	0.390977
2.35	28393	23775	0.322853	0.385551
2.3909	35000	29308	0.311960	0.372542
2.3522	45000	37682	0.298500	0.356469
2.2903	55000	46056	0.287869	0.343776
2.2266	65000	54430	0.279184	0.333401
2.1664	75000	62804	0.271880	0.324679

Table C-5
 Neutral Stability Results for $n=1.0$ at
 $\chi=0.007$, $U_{\max}=1.21157$, $N=150$

α	R	R*	(c_r)	$(c_r)^*$
1.70	25591	21122	0.318671	0.386092
1.80	24690	20378	0.322468	0.390693
1.895	24353	20100	0.324831	0.393555
1.90	24360	20106	0.324897	0.393635
2.00	24804	20472	0.325432	0.394284
2.10	27139	22399	0.321846	0.389939

Table C-6
 Neutral Stability Results for $n=1.0$ at
 $\chi=0.009$, $U_{\max}=1.24367$, $N=150$

α	R	R*	(c_r)	$(c_r)^*$
1.40	26597	21386	0.310225	0.385818
1.50	25190	20255	0.315206	0.392012
1.5930	24674	19840	0.318163	0.395690
1.60	24686	19850	0.318267	0.395819
1.70	25574	20564	0.318155	0.395680

Table C-7
 Neutral Stability Results for $n=1.0$ at
 $\chi=0.010$, $U_{\max}=1.25870$, $N=100$

α	R	R*	(c_r)	$(c_r)^*$
0.70	69543	55250	0.252730	0.318111
0.80	55767	44306	0.262914	0.330930
1.00	38808	30832	0.282568	0.355668
1.20	29928	23777	0.299456	0.376925
1.40	25874	20556	0.311265	0.391789
1.475	25426	20200	0.313713	0.394871
1.500	25548	20297	0.313940	0.395156
1.600	27700	22007	0.311407	0.391969
1.6257	30000	23834	0.307564	0.387131
1.6342	35000	27806	0.299566	0.377064
1.6005	45000	35751	0.286198	0.360237
1.5530	55000	43696	0.275636	0.346943
1.5058	65000	52435	0.266979	0.336046
1.4617	76000	59585	0.259700	0.326884

Table C-8
 Neutral Stability Results for $n=1.0$ at
 $\chi=0.015$, $U_{\max}=1.32702$, $N=100$

α	R	R*	(c_r)	$(c_r)^*$
0.55	74047	55799	0.249865	0.331576
0.60	65463	49331	0.254373	0.337558
0.70	52531	39586	0.263511	0.349684
0.80	43790	32999	0.272244	0.361273
0.90	38117	28724	0.279851	0.371368
0.95	36308	27361	0.282881	0.375389
1.00	35241	26557	0.285077	0.378303
1.025	35060	26420	0.285713	0.379147
1.050	35246	26560	0.285827	0.379298
1.100	38250	28824	0.282474	0.374849
1.1101	45000	33911	0.274538	0.364317
1.0896	55000	41446	0.264516	0.351018
1.0608	65000	48982	0.256263	0.340066
1.0314	75000	56518	0.249329	0.330865

Appendix D
 Tables of Neutral Stability Characteristics at
 Critical Point

Table D-1

Axial Variation of Critical Stability Characteristics for
 Axisymmetric Disturbances $n=0$

χ	X	α_c	R_c^*	R_c	$(c_r)_c^*$	$(c_r)_c$	N
0.002	0.00087	4.19	30110	33338	0.366582	0.331058	200
0.003	0.00140	3.28	24620	27897	0.380775	0.336043	200
0.005	0.00258	2.26	20380	23960	0.403796	0.343469	150
0.006	0.00323	1.93	19900	23765	0.413491	0.346250	150
0.007	0.00392	1.635	20250	24534	0.422166	0.348445	150
0.009	0.00539	1.095	25015	31110	0.434888	0.349683	150
0.010	0.00616	0.785	33840	42594	0.437008	0.347191	100

Table D-2
 Axial Variation of Critical Stability Characteristics
 for Non-Axisymmetric Disturbances $n=1.0$

χ	X	α_c	R_c^*	R_c	$(c_r)_c^*$	$(c_r)_c$	N
0.002	0.00087	4.135	31510	34888	0.363319	0.328136	200
0.003	0.00140	3.240	26220	29710	0.373960	0.330029	200
0.005	0.00258	2.363	21780	25605	0.386854	0.329058	150
0.006	0.00323	2.103	20700	24720	0.390977	0.327397	150
0.007	0.00392	1.895	20100	24353	0.393555	0.324831	150
0.009	0.00539	1.593	19840	24674	0.395690	0.318163	150
0.010	0.00616	1.475	20200	25426	0.394871	0.313713	100
0.015	0.01043	1.025	26420	35060	0.379147	0.285713	100